



Reference: 417034.200

March 5, 2018

Mr. Joe Miller, PE
SCS Engineers
3843 Brickway Blvd. Suite 208
Santa Rosa, CA 95403

**Subject: Geologic and Seismic Siting Assessment for the Proposed Eastlake Landfill
Expansion, Lake County, California**

1.0 Introduction

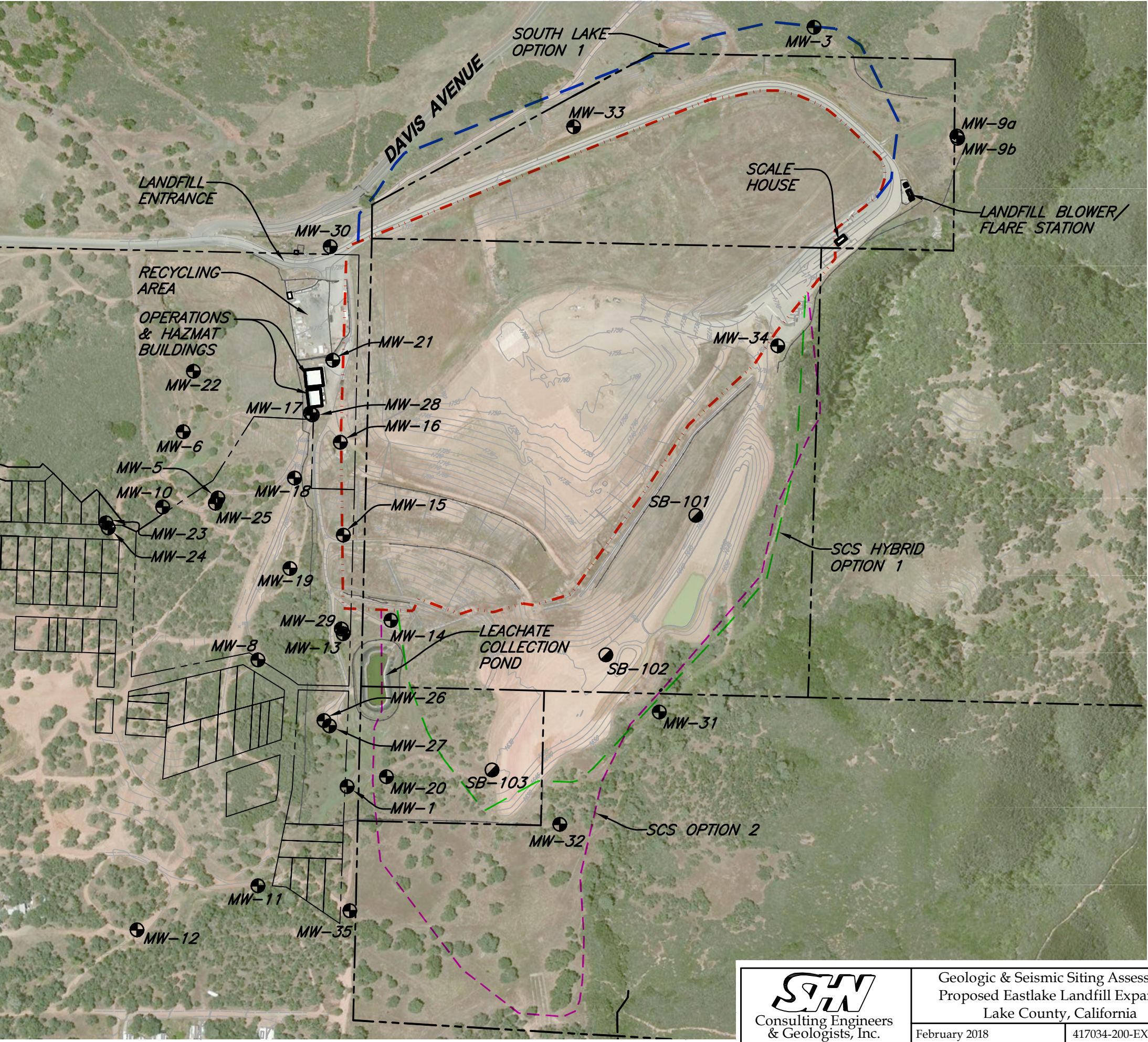
The following report summarizes the geologic and seismic conditions at the Eastlake Landfill pertaining to compliance with regulatory requirements for the proposed Eastlake Landfill expansion and future cell construction. The existing landfill property encompasses five (5) separate parcels owned by the County of Lake totaling 80 acres of which 34 acres are currently permitted for Class III waste disposal. Existing facilities at the site include a scale and gatehouse, maintenance and operation buildings, leachate collection pond, a gas blower and flare station, and surface water impoundment (Figure 1). To date, a network of 35 groundwater monitoring wells have been installed at the facility.

Former and current waste emplacement occurs within a south-southwest trending canyon. Cover material for the existing refuse areas is generated onsite from a borrow area located to the south of the permitted refuse area. Areas being considered for development as part of the landfill expansion primarily include the previously disturbed borrow area as well as currently undeveloped land to the south of the borrow area, and land abutting the north edge of the of the currently permitted refuse area.

1.1 Proposed Expansion Plans

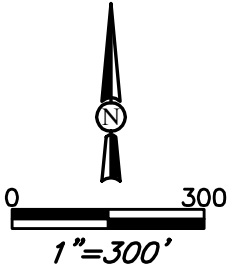
The proposed landfill expansion and future waste cell construction will include a new Subtitle D-compliant waste disposal cell potentially in the existing borrow area and in the undeveloped area located on the southernmost parcel. Additional areas being considered include the area north of the currently permitted refuse area. All proposed expansion areas are shown on Figure 1 and labeled as SCS Hybrid Option 1, South Lake Option 1, and SCS Option 2. Base grading plans, liner details, leachate collection system details, and gas collection system details for the proposed waste cell are currently being prepared by SCS Engineers but have not been provided as of the date of this report. Because the site is being proposed as a Class III landfill expansion for nonhazardous solid waste, it is subject to the geologic and seismic siting criteria specified in Section 20260 Title 27 of the California Code of Regulations.

\\Eureka\Projects\CAD-FILES\Willits\2017\417034-EASTLAKE\417034-200, SAVED: 2/13/2018 4:30 PM CNEWELL, PLOTTED: 2/13/2018 4:31 PM, CHRIS D. NEWELL



NOTE:
1. BASE MAP A COMBINATION OF
PARCEL LINES FROM LAKE COUNTY,
AERIAL SURVEY FROM SCS
ENGINEERS, "SITE PLAN," DATED
09-26-17, AND SURVEY DONE BY
SHN ENGINEERS, 2017

- EXPLANATION**
- PARCEL LINE
 - MONITORING WELL LOCATION AND DESIGNATION
 - GEOTECHNICAL BORING LOCATION AND DESIGNATION
 - - - - - APPROXIMATE PERMITTED REFUSE LIMIT
 - - - - - SCS HYBRID OPTION 1 (EXTENT OF FILL)
 - - - - - SOUTH LAKE OPTION 1 (EXTENT OF FILL)
 - - - - - SCS OPTION 2 (EXTENT OF FILL)
 - 1700- EXISTING TOPOGRAPHIC CONTOUR IN FEET



SH
Consulting Engineers
& Geologists, Inc.

Geologic & Seismic Siting Assessment
Proposed Eastlake Landfill Expansion
Lake County, California
February 2018

Existing Site Conditions
SHN 417034.200
Figure 1

1.2 Purpose and Scope of Geologic and Seismic Assessment

The primary purpose of SHN's desktop and field investigation was to review available geologic data for the site and evaluate the proposed new waste cell locations with respect to Class III landfill siting criteria as specified in Title 27. Primary addressed in this report is a characterization of the site pertaining to the potential for surface fault rupture and rapid geologic change to directly affect the proposed expansion areas. The scope of work completed to address the seismic and rapid geologic change criteria included the following:

- A desktop review of existing site data including published geologic mapping, fault activity maps, and the epicenter locations of recorded historic seismicity available from the United States Geological Survey (USGS) and California Geological Survey (CGS);
- Review of existing subsurface exploration boreholes previously drilled at the site for the installation of monitoring wells;
- Additional subsurface investigation including the drilling of five boreholes with downhole geophysical logging performed on two of the boreholes.
- A seismic refraction survey to image the locations of suspected bedrock faults projecting through the proposed expansion area;
- Preparation of this report with findings and conclusions pertaining to fault activity and the potential for rapid geologic change. SHN has also provided a discussion of the soil rippability based on the downhole geophysical logging and seismic refraction survey.

2.0 Conformance with Geologic and Seismic Siting Criteria

The new cells proposed for the landfill expansion are planned Class III waste disposal cells. Pursuant to the regulations specified in Section 20260 Title 27, they are subject to the geologic and seismic siting criteria outlined below and addressed in the following sections:

- Surface Ground Rupture - New Class III and expansions of existing Class II-2 landfills shall not be located on a known Holocene fault.
- Rapid Geologic Change - New Class III landfills can be located within areas of potential rapid geologic change only if the RWQCB finds that the unit's containment structures are designed, constructed, and maintained to preclude failure.

As described in detail below, the results of our assessment indicate that the areas proposed for landfill expansion meet the Title 27 siting criteria and are determined to be suitable for future development as Class III waste disposal areas.

2.1 Fault Siting Criteria

Active faults are defined as faults that have had surface displacement in the Holocene epoch (in the past 11,000 years) based on CCR Division 2, Title 14, also known as the Alquist-Priolo Earthquake Fault Zoning Act (A-P Act). Potentially active faults are defined by the A-P Act as faults showing surface displacement during mid to late Quaternary time (about 1.6 million years before present) that have a relatively high potential for ground rupture. In general, Quaternary faults that do not record evidence of Holocene surface displacement are not considered as being active by the State of California.

Regional and Local Faults

Based on the most recent available data, no active or potentially active faults are reported to be present within the boundaries of the project site (Figure 4). The Eastlake Landfill is not located within an A-P Earthquake Fault Hazard Zone (CDMG, 1982; CDMG, 1983; Jennings, 2010). Regional active faults within about 50 miles of the Eastlake Landfill include the Konocti Bay fault zone, Big Valley fault, Hunting Creek-Berryessa fault, the north section of the Maacama fault zone, San Andreas fault, Bartlett Springs fault (Bryant and Hart, 2007) and Great Valley 03 Mysterious Ridge blind thrust fault (USGS and CGS, 2018). In addition to the regional active faults, multiple unnamed and early Quaternary faults have been identified within the limits of the proposed northern and southern landfill expansion areas as depicted on Figure 2 (Hearn and others, 1995). None of these faults, however, are zoned as Holocene-active faults by CGS. The most recent fault activity map of California (Figure 3; Jennings, 2010) indicates the local faults are less than 1.6 million years old but lack evidence of movement in the middle to late Quaternary (i.e. the last 700,000 years).

Hearn and others (1976) mapped the Clear Lake area in detail and depict an extremely complex pattern of faults (Hearn and others, 1995). From their mapping, they concluded that the Clear Lake area fits a system of deformation related to northwest-directed right-lateral strike-slip faulting that has locally been overprinted by features related to Quaternary volcanism. Subsequent researchers (Herd, 1982) suggested that faults in the Clear Lake area are primarily related to caldera subsidence and formation of the Clear Lake basin. SHN therefore interprets the identified local bedrock faults to be a product of earlier geologic processes which are no longer active in the areas proximal to the Eastlake Landfill. SHN found no evidence during our field reconnaissance and aerial imagery review suggestive of active faulting such as linear escarpments, vegetation lineaments, offset drainages, or offset ridges indicating that the faults crossing the facility are relict structures which are no longer capable of surface fault rupture.

The nearest Holocene age fault to the Eastlake Landfill is the seismically active Konocti Bay fault zone located 5 miles to the southwest at its closest point to the site (Figure 4). The Konocti Bay fault zone is comprised of multiple discontinuous fault segments that strike north-northwest to north-northeast and are located south and east of Mt. Konocti (CDMG, 1982; CDMG, 1983). The fault zone ranges in width from about 1,500 feet to 10,000 feet. Readily evident displacements identified from field reconnaissance and aerial photographic analysis is mainly normal. Geomorphic features suggestive of Holocene activity such as backfacing scarps, sidehill benches, deflected drainages, and offset ridges are abundant along the principal northwest-trending faults. Focal-plane solutions from historic seismicity attributed to the Konocti Bay fault zone indicate strike-slip motion to be the primary fault mechanism at depth. Holocene age faulting is further attested to by the presence of a fault lineament beneath Konocti Bay, which is marked by a prominent line of gaseous springs that records displacement recent enough to have produced a 1 meter high scarp preserved in the lake bottom sediments.

Table 1 summarizes the maximum probable earthquake (MPE) associated with regional active faults located within 25 miles of the site. The MPE is the design earthquake for Class III landfills, is typically defined as the maximum earthquake likely to occur in a 100-year period, and shall not be less than the maximum historical event. As shown in Table 1, the MPE for the listed faults in proximity to the Eastlake Landfill are capable of generating estimated peak horizontal ground accelerations (PHGA) of up to 0.7 g at the site (USGS, 2013).

EXPLANATION

- al

Alluvium (Holocene)—Flood-plain, channel, and lake deposits of clay, silt, sand, and gravel. Locally may include youngest part of the basin deposits of Clear Lake (bcl)
- co

Colluvium (Holocene)—Slope deposits of silt, sand, and coarser angular clasts. Mapped only where extensive or where covers critical contact of bedrock units
- ls

Landslide deposits (Holocene and Pleistocene)—Unsorted angular blocks and soil. Largest landslide deposit is on the west side of Mount Konociti; consists of the dacite of Benson Ridge (dbr) and rhyodacite of Soda Bay (dsb) and has an inferred maximum thickness of at least 250 m. Contact between adjacent landslide deposits on map separates landslides of different age or direction of movement
- dhi

Dacite of Clearlake Highlands (Pleistocene)—Flows of moderately porphyritic dacite; lacks diabasic-textured mafic inclusions. Interbedded with and overlain by the Lower Lake Formation (ll). Age of 0.52±0.06 Ma. Maximum exposed thickness 50 m
- ll

Lower Lake Formation (named by Rymer, 1981; includes basin deposits of Wildcat Canyon of Hearn and others, 1976) (Pleistocene)—Lacustrine, marsh, fluvial, pyroclastic, and volcanoclastic deposits in an ancestral Clear Lake basin. West of and at Lower Lake, composed of dominantly sandstone and siltstone and lesser amounts of claystone, diatomaceous siltstone, conglomerate, and tuff; conglomerate contains pebbles and cobbles of chert, andesite, dacite, the rhyodacite of Diener Drive (dd), and, rarely, obsidian. Near Lower Lake, unit contains beds of pebbly fossiliferous limestone up to 1 m thick and numerous beds of tuff and lapilli tuff of mafic to silicic composition up to 1.3 m thick (Rymer, 1981). North of Lower Lake, unit contains siliceous siltstone and mudstone, which commonly have root casts and diatom and gastropod fossils, and also contains 0.3–3-m-thick beds of orange limonitic mudstone that are especially prominent within Redbank Gorge, 0.5–2-m-thick beds of tan to gray, surge-like lapilli tuff of basaltic andesite, and rare beds of carbonaceous mudstone. Unconformably overlies the Cache Formation (QTc); adjacent to and overlies the rhyodacite of Diener Drive (dd); interbedded with and overlies the dacite of Clearlake Highlands (dhi); overlain by the dacites of Thurston Lake (dt), Pinkeye Lake (dpl), and Cache Creek (dcc), and flow (brf) of the basaltic andesite of Roundtop Mountain. Probable age range from 0.4 to 0.65 Ma. Thickness 0–25 m in upper Wildcat Canyon, thickness of tilted sequence at Lower Lake at least 200 m, exposed thickness in Redbank Gorge 20 m
- beu

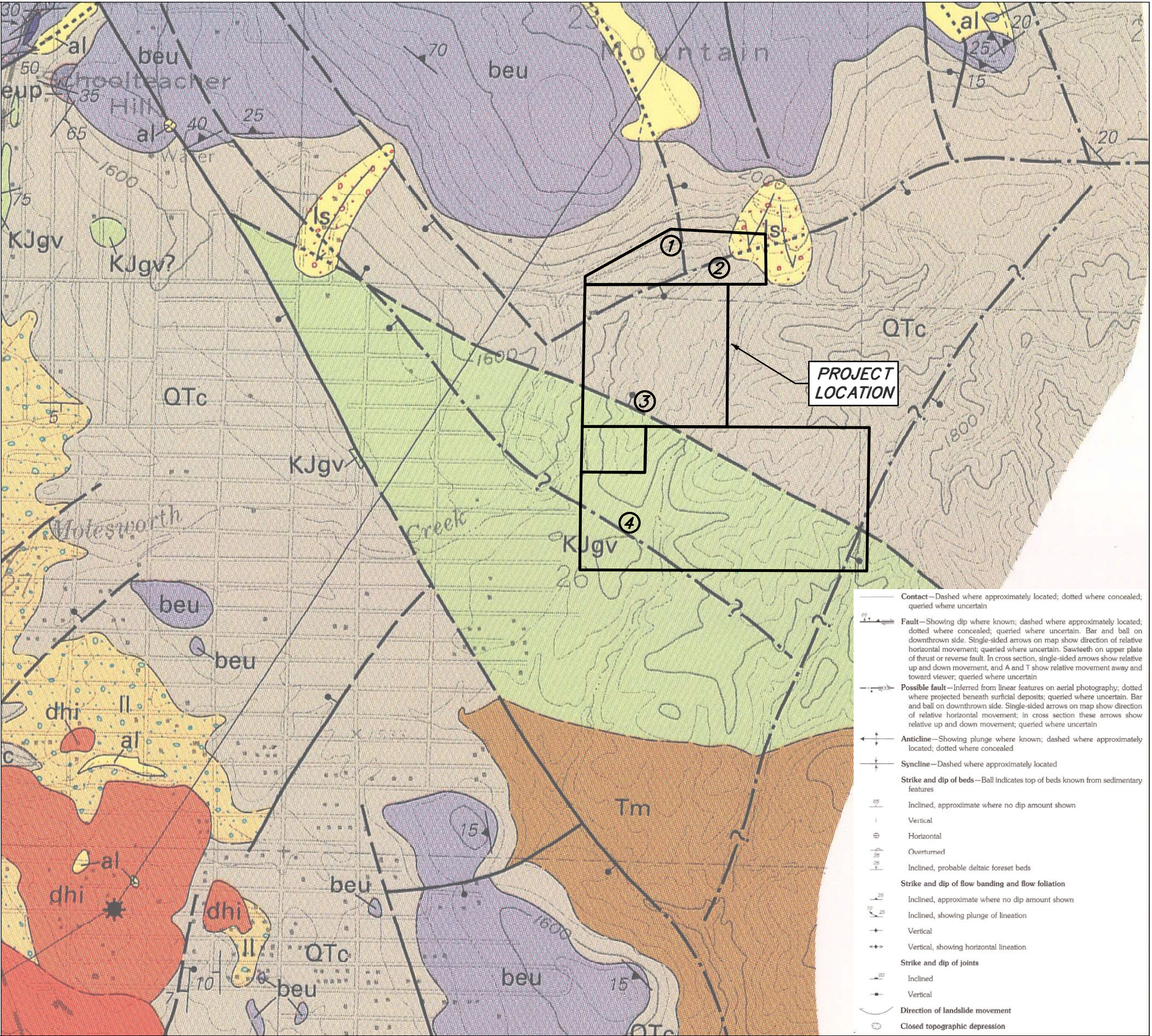
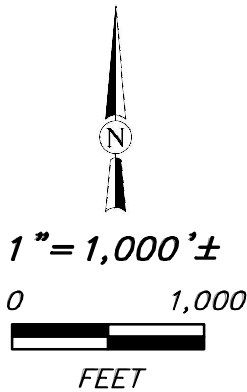
Undivided—Dominantly flows; lesser pyroclastic deposits and intrusive rocks
- beup

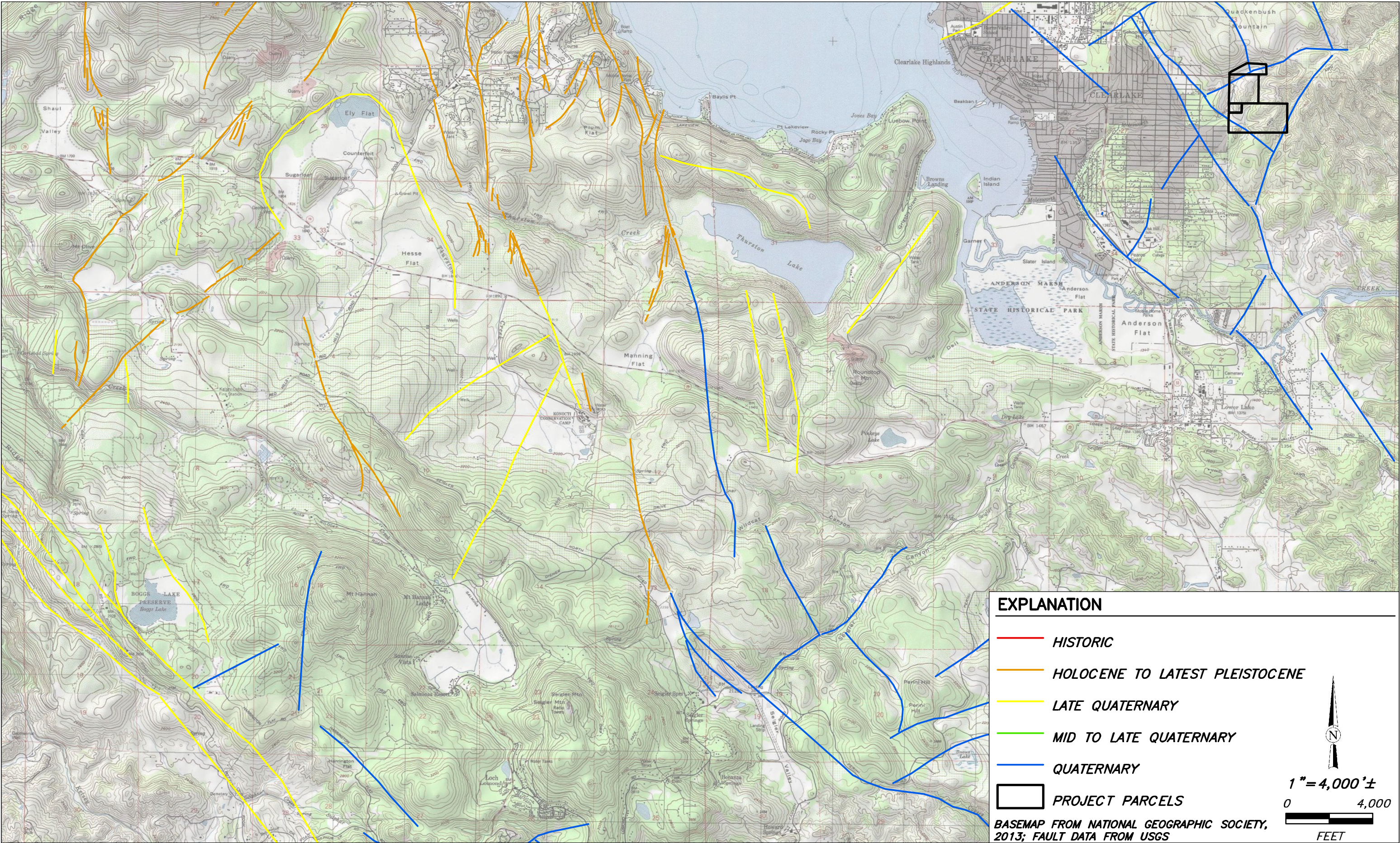
Pyroclastic deposits—Bomb, block, and lapilli tephra, pyroclastic breccia, lapilli tuff
- QTc

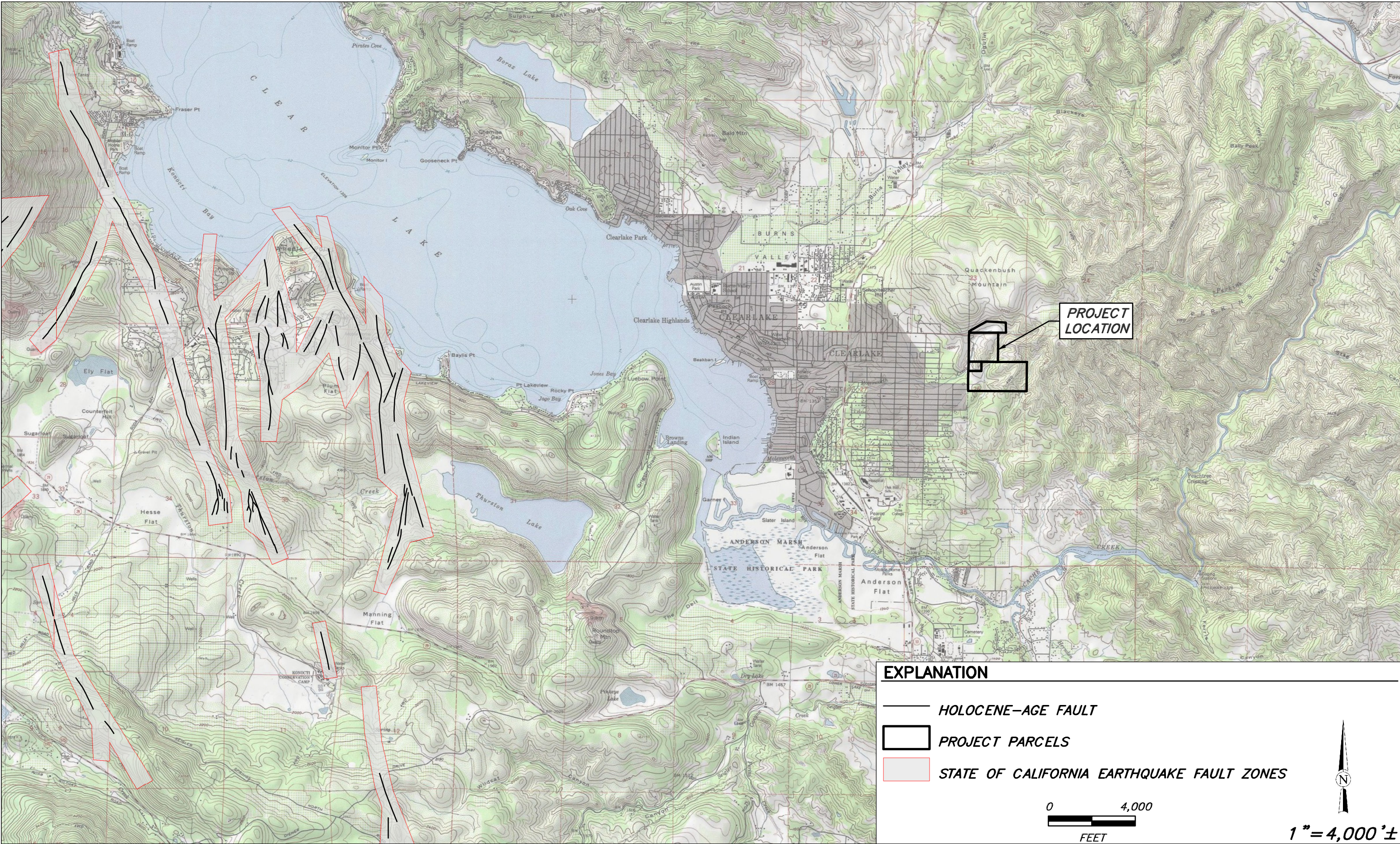
Cache Formation (revised by Rymer, 1981) (Pleistocene and Pliocene)—Siltstone, sandstone, conglomeratic sandstone, and tuff. Fluvial and locally lacustrine origin; deposited in fault-bounded basin that is older than and separate from the Clear Lake basin. In map area, contains 5–15 percent of 1–5-cm-diameter pebbles mainly of chert, vein quartz, and greenstone, and contains 1 percent or less of pebbles of graywacke, shale, and serpentinite. Contains late Pliocene mammalian fossils (Rymer, 1981). Blackeye Canyon section (Rymer, 1981) contains rhyolitic(?) tuff as much as 3.5 m thick and lapilli tuff and pyroclastic breccia (beup) of the early basaltic rocks unit as much as 2.7 m thick. Generally lacks pebbles of the Clear Lake Volcanics, except from the early basaltic rocks units (beu, beup) from nearby sources. See Anderson (1936), Brice (1953), and Rymer (1981) for more detailed descriptions of this unit. Forms dissected topography with grass-covered slopes and lag gravel on the surface. Probably derived mainly from the north and east. As mapped here, the upper part contains interbedded early basaltic rocks (beu) near Clearlake Highlands, and the lower or middle part contains interbedded and intrusive early basaltic rocks (beui, beu) near the Bartlett Springs fault zone; also intruded by and overlain by the early basaltic rocks (beu, beup, beui). Age of unit is late Pliocene and early Pleistocene (Rymer, 1981). Maximum thickness unknown, but minimum thickness is 1,600 m (Rymer, 1981)
- Tm

Martinez Formation (Paleocene)—Marine sandstone and lesser amounts of mudstone and conglomerate; see Brice (1953) and Swe and Dickinson (1970) for further description
- KJgv

Great Valley sequence (Upper Cretaceous to Upper Jurassic)—Shale, siltstone, graywacke, conglomerate, greenstone, and chert. See Brice (1953), Swe and Dickinson (1970), and McLaughlin and others (1990) for more detailed descriptions and subdivisions of this unit







DATA SOURCE: EARTHQUAKE FAULT ZONES:
CLEARLAKE HIGHLANDS QUADRANGLE (CDMG, 1983)



Geologic & Seismic Siting Assessment
Proposed Eastlake Landfill Expansion
Lake County, California

Earthquake Fault Zones
Map
SHN 417034.200

February 2018

Figure4_FaultMap

Figure 4

Table 1 Summary of Active Faults in Proximity to Eastlake Landfill					
Fault Name	Style of Faulting	Distance From Landfill		MPE ² Magnitude (M _w) ³	MPE PHGA ⁴ (g) ⁵
		miles	km ¹		
Konocti Bay Fault Zone	Strike-slip	5	8	unknown	0.55
Hunting Creek-Berryessa Fault Zone	Strike-slip	10	17	6.9	0.46
Great Valley 03 Mysterious Ridge	Reverse	15	24	7	0.56
Maacama	Strike-slip	23	37	7.1	<0.7
Bartlett Springs	Strike-slip	23	37	7.1	<0.7
1. km: kilometers 2. MPE: maximum probable earthquake 3. Mw: moment magnitude 4. PHGA: peak horizontal ground acceleration 5. g: acceleration due to gravity					

2.1.2 Project Site Fault Assessment

Several bedrock fault structures of Quaternary age have been identified within the northern and southern limits of the proposed landfill expansion areas (Hearn and others, 1995). These faults include: 1) the two unnamed faults trending north and northeast in the northern parcel located within the "South Lake Option 1" landfill expansion area, and 2) the two unnamed faults trending northwest through the existing borrow area and undeveloped lands south of the borrow area located within the "SCS Hybrid Option 1" and "SCS Option 2" landfill expansion areas. The identified fault traces are shown on Figure 2 and labeled numbers 1 through 4. Fault trace number 3 shown on Figure 2 has been omitted on the State of California Fault Activity Map and is therefore not included on Figure 3. The fault is presumably considered to be pre-Quaternary age due to its omission on the State's Fault Activity Map, which depicts all known Quaternary faults in California.

Fault traces #1 and #2 within the proposed northern expansion area are projected to underlie the existing permitted waste cell as does fault trace #3 in the proposed southern expansion area. None of these fault structures are judged to have been active during the Holocene, nor are they considered capable of surface ground rupture for the reasons outlined below.

- Unnamed fault trace #1:** This fault trace enters the northern boundary of the existing permitted landfill waste cell, and trends north to north-northwest. The sense of movement on the fault is reportedly normal with a down-to-the-east sense of displacement. The existing topography and geomorphic expression of Quackenbush Mountain, which is bisected by fault trace #1, currently displays higher relief to the east side of the fault which is opposite the sense of displacement. This fault is attributed by Herd (1982) to be primarily the result of constructional volcanic processes and local caldera collapse which are unlikely to constitute a future hazard. The displacements along these faults are thought to represent a one-time event, with little chance of recurring displacement. We therefore interpret the existing topography to be a product of landscape erosion and not active faulting. We conclude that fault trace #1 is early Quaternary in age and has not exhibited movement during the late Quaternary or Holocene time. SHN therefore judges the potential for movement to recur in the future on this fault trace to have a very low probability.

- **Unnamed fault trace #2:** The fault trace enters the northwest boundary of the currently permitted waste cell and is located within the limits of the proposed northern expansion area. The fault trends northeast and dips to the southeast. The sense of movement on the fault is reportedly normal with a down-to-the-southeast sense of displacement, and is confined to the Tertiary to Quaternary age Cache Formation. The portion of the fault trace within the northeast corner of the expansion area is concealed by a Pleistocene to Holocene age landslide deposit. Concealment of the fault trace by the landslide deposit indicates that the most recent fault movement predates the deposit. The most recent age of faulting is therefore interpreted to be pre-Holocene based on stratigraphic relations. The fault trace could not be located in the field within any certainty during our field reconnaissance and evaluation of aerial imagery. Northeast of the project site boundary the fault trace is cross-cut by two deeply incised southward flowing drainages with no preserved scarps being evident. Topography further to the northeast along the fault trace indicates the ground slopes to be opposite the sense of fault displacement indicating the landscape to be a product of erosion and not active faulting. SHN therefore judges the potential for movement to recur in the future on this fault trace to have a very low probability.
- **Unnamed fault trace #3:** The fault trace projects through the boundaries of the currently permitted waste cell and is located within the eastern limits of the proposed southern expansion area. The fault trends northwest and dips to the northeast. Stratigraphic and structural relations indicates the fault to have a down-to-the-northeast normal sense of displacement and emplaces Tertiary to Quaternary age conglomerate of the Cache Formation over Cretaceous to Jurassic age sandstone of the Great Valley sequence. The fault is partially exposed in the vicinity of borehole SB-102 in the east-facing cut-slope created during grading of the road accessing the borrow area. Exposure of the fault zone is also observed in an east-facing cut slope in the vicinity of monitoring well MW-19 on the west side of the permitted waste cell. Stratigraphic relations from borehole data collected from borings SB-102 and SB-101 indicate the basal contact of the Cache Formation with the Great Valley sequence to be offset down-to-the-northeast a minimum of 25 feet across the fault. The seismic refraction conducted as part of this investigation imaged the fault displacement near the location of Station 500 where 20 to 30 feet of down-to-the-north displacement of the Great Valley sequence bedrock is evident. Topography along the fault trace indicates the ground slopes on a landscape-scale to be opposite the sense of fault displacement. We therefore interpret the current south-facing landscape to be a product of stream incision and land surface erosion. The location and sense of displacement of fault trace #3 is not controlling the existing surface morphology. SHN therefore judges the potential for movement to recur in the future on this fault trace to have a very low probability.
- **Unnamed fault trace #4:** This fault trace which is queried on the most recent geologic maps projects through the southernmost limits of the proposed southern expansion area. The fault trends northwest and dips to the southwest. The sense of movement on the fault is reportedly normal with a down-to-the-southwest sense of displacement, and is confined to the Cretaceous to Jurassic age Great Valley sequence. Stratigraphic relations from borehole data collected from borings SB-103 and MW-35 indicate the basal contact of the sandstone unit with the underlying siltstone within the Great Valley sequence to be offset down-to-the-southwest a minimum of 90 feet across the fault. Alternatively, the apparent displacement between the two exploration locations may be a product of the southwest dipping bedding identified in SB-103 from the borehole televiewer. Topography along the fault trace in the vicinity of MW-35 indicates the ground slopes to

be opposite the sense of fault displacement. South of the mapped fault trace the ground surface is observed to slope to the north toward an unnamed drainage swale. Field reconnaissance of the undeveloped areas to the west of the facility revealed no geomorphic evidence suggestive of active faulting such as youthful appearing fault scarps or deflected drainages. SHN therefore judges the potential for movement to recur in the future on this queried fault trace to have a very low probability.

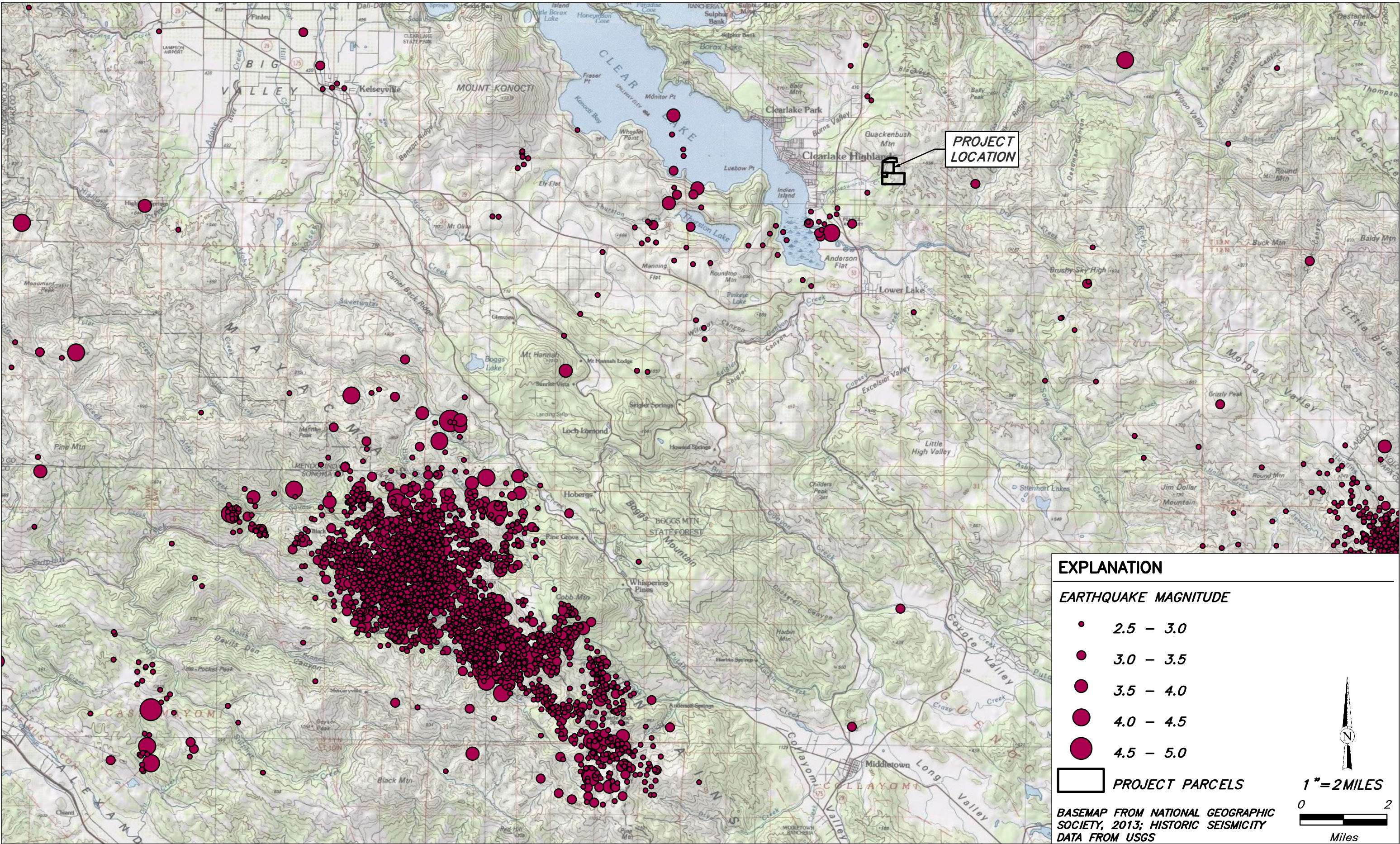
2.1.2 Evaluation of Seismic Activity

Historic seismicity data were reviewed to evaluate whether measurable seismic activity may have occurred within or near the Eastlake Landfill on the identified unnamed faults that project through the site. This assessment was performed using a data base assembled by the Northern California Earthquake Data Center and accessed through the United States Geological Survey historic seismicity database. All recorded historic earthquakes with a magnitude greater than 2.5 were plotted in relation to the project site as depicted on Figure 5. The results of this evaluation indicate that no historic seismic or microseismic activity has been recorded within the Eastlake Landfill boundaries. Therefore, SHN judges the potential for Holocene active faults to be located within 200 feet of the proposed landfill expansion areas to be unlikely.

3.0 Soil Rippability

Data acquired from the borehole geophysical logging (Appendix 1) and seismic refraction survey (Appendix 2) conducted by Norcal Geophysical Consultants were used to evaluate the depth, variability and rippability characteristics of the subsurface bedrock material and to assist in the landfill expansion design criteria. A single seismic line with a length of 1,260 feet was acquired using five overlapping spreads. Each spread was composed of 24 geophones and 5 shot points distributed in a collinear array. The distribution of the geophones and shot points resulted in a total length of 300 feet for each spread. The seismic line was located in the existing borrow area and access road encompassing boreholes SB-101 through SB-103 as shown on Plate 1 of Appendix 2.

In general, bedrock at the site is characterized as moderately to intensely weathered with seismic velocities of 4,000 to 9,000 feet per second (ft/sec). In the southern portion of the existing borrow area, bedrock materials ranging in velocity from 3,000 to 8,000 ft/sec occur to a depth of 45 feet below the existing ground surface corresponding to an elevation of about 1,580 feet. The 8,000 ft/sec velocity contour ascends to the north to an elevation of about 1,610 feet.



Path: \\eureka\projects\GIS-Files\Wlilts\2017\417034\200_Eastlake\F\PROJ_MXD\Figure5_HistoricSeismicityMap.mxd

Based on rippability charts published by Caterpillar Tractor Co., sandstone bedrock, such as the Great Valley sediments underlying the site, are generally considered marginal to rip with a D9 or equivalent in the compression wave velocity range of 7,500 to 9,500 ft/sec. Based on this information, a range of excavation to subgrade up to about 50 feet below the existing ground surface may be attainable using the existing heavy equipment at the facility.

SHN Engineers & Geologists



Giovanni A. Vadurro, CEG
Engineering Geologist



- Appendices: 1. Borehole Geophysical Logging Investigation (Norcal Geophysics, 2017)
2. Seismic Refraction Survey (Norcal Geophysics, 2018)

Reference Cited

- Bryant, W.A. and E.W. Hart. (2007). "Fault-Rupture Hazard Zones in California, Alquist-Priolo Earthquake Fault Zoning Act with Index to Earthquake Fault Zones Maps. Special Publication 42.
- Bryant, W.A. (1982). "Fault Evaluation Report-Konocti Bay Fault, Collayomi Fault, Big Valley Fault, and other Unnamed Fault Segments in the Clear Lake Area," California Department of Conservation, Division of Mines and Geology FER-132, 16 p.
- California Division of Mines and Geology. (1982). "Fault Evaluation Report FER-132, Konocti Bay Fault, Collayomi Fault, Big Valley fault, and Other Unnamed Fault Segments in the Clear Lake Area, California." Sacramento, CA: CDMG.
- California Division of Mines and Geology. (1983). "State of California Special Studies Zones, Clearlake Highlands Quadrangle, Official Map, California," James F. Davis, State Geologist, Department of Conservation. NR:CDMG.
- Hart, E. W., W. A. Bryant, and T. C. Smith. (1983). "Summary Report--Fault Evaluation Program, 1981-1982 Area, Northern Coast Ranges region, California." California Department of Conservation, Division of Mines and Geology Open-File Report 83-10, 17 p., 1 pl.
- Hearn, B.C., J.M Donnelly-Nolan, and F. E. Goff. (1976). "Preliminary Geologic Map and Cross-section of the Clear Lake Volcanic Field, Lake County, California." U.S. Geological Survey, Open-File Map 76-751, scale 1:24,000.
- Hearn, B.C., J.M Donnelly-Nolan, and F. E. Goff. (1995). "Geologic Map and Structure Sections of the Clear Lake Volcanics, Northern California." U.S. Geological Survey, Miscellaneous Investigations Series, Map I-2362.
- Herd, D.G. (1982). "Map of Principal late-Quaternary faults, San Francisco Bay Region, California." U.S. Geological Survey, Miscellaneous Field Studies, scale 1:250,000.

Jennings. (2010). Fault Activity Map of California, California Geological Survey Geologic Data Map No. 6," compilation and interpretation by Charles W. Jennings and William A. Bryant. Accessed February 2018 at: <http://www.quake.ca.gov/gmaps/FAM/faultactivitymap.html>

United States Geological Survey. (2013). "2008 National Seismic Hazard Map Program Probabilistic Seismic Hazard Analysis Interactive Deaggregations," U.S. Department of the Interior, Accessed May 2015, from USGS web site: <http://geohazards.usgs.gov/deaggint/2008/documentation.php>

United States Geological Survey and California Geological Survey. (2018). "United States Quaternary Fault and Fold Database for the United States." Accessed February 2018, from USGS web site: <https://earthquake.usgs.gov/hazards/qfaults/>

1

Borehole Geophysical Logging Investigation

February 19, 2018

SHN Consulting Engineers & Geologists, Inc.
812 W. Wabash Ave.
Eureka, CA 95501

Subject: Borehole Geophysical Logging Investigation
Eastlake Landfill
Lake County, California
NORCAL Job No. NS175076

Attention: Mr. Erik Nielson

This report presents the findings of a borehole geophysical logging (BGL) investigation performed by NORCAL Geophysical Consultants, Inc. for SHN Consulting Engineers & Geologists, Inc. (SHN) at the subject facility. The BGL investigation is in support of an on-going geotechnical investigation being conducted by SHN for a potential landfill expansion. The BGL field work was conducted on December 22, 2017 by NORCAL California Professional Geophysicist William J. Henrich (PGP No. 893). Mr. Giovanni Vadurro, SHN Project Geologist, provided background information and direct field assistance.

1.0 SCOPE OF WORK

Our scope of work consisted of conducting a BGL investigation in two boreholes labeled B-102 and B-103. The locations of the boreholes are shown in Figure 1. The BGS investigation consisted of the following surveys:

- Borehole Caliper (BC)
- Natural Gamma (NG)
- Electromagnetic Induction (EMI)
- Suspension Borehole Logging (SBL)
- Borehole Televier (BHTV)

The SBL survey was to be conducted in the deepest borehole only (B-103) in order to provide compressional (P-) wave velocity information in advance of a proposed seismic refraction survey. We were also tasked with processing, analyzing and interpreting the BGL data and presenting our findings in a written report.



2.0 OBJECTIVES

The objectives of the BGL survey were as follows:

1. Identify variations in the subsurface lithology,
2. Measure P-wave velocities in B-103
3. Map fracture distribution in B-102 and B-103

It is our understanding that this information will be used to characterize the geology, provide estimates of bedrock P-wave velocity and to characterize the degree of bedrock fracturing and, where applicable, determine bedding attitudes.

3.0 LOCAL GEOLOGY

The primary stratigraphic units underlying the project site from oldest to youngest include the Upper Cretaceous to Upper Jurassic Great Valley sequence and Plio/Pleistocene age Cache Formation. The Great Valley sequence consists of strongly indurated marine sediments composed of shale, graywacke, conglomerate, greenstone, and chert. Cache Formation consists predominantly of fluvial and lacustrine sediments composed of poorly indurated siltstone, sandstone, and conglomeratic sandstone deposited within an inter-montane basin that predates the current Clear Lake basin. The lithologic unit encountered in boreholes B-102 and B-103 are interpreted to represent thickly bedded siltstone and sandstone of the Great Valley sequence.

4.0 BOREHOLE CONDITIONS

The approximate locations of the Boreholes B-102 and B-103 are shown in Figure 1. Both boreholes were drilled with rotary PQ drilling methods that produces a 5-inch diameter borehole. The boreholes ranged in depth from 43 to 77 feet below ground surface (bgs), respectively. The water level in the boreholes varied from 40 feet bgs in B-103 to no groundwater encountered to a total depth at 43 feet in B-102. We added water to both boreholes prior to the SBL and BHTV surveys because these tools require a fluid column to operate. Both boreholes were prone to sloughing having lost several feet of depth before the commencement of geophysical logging.

5.0 BOREHOLE GEOPHYSICAL LOGGING METHODS

Detailed descriptions of the methodology, data acquisition and data analysis procedures for the various BGL techniques are presented in Appendix A. Also included is a table listing the seismic velocities measured in B-103 (SBL survey) and Discontinuity Tables listing the fracture analysis

results of the televiwer surveys conducted in both boreholes. Graphical plots showing the unwrapped televiwer images, the borehole diameter trace, the dips analysis, the rewrapped core image and the borehole inclination traces for both boreholes are presented in Appendix B.

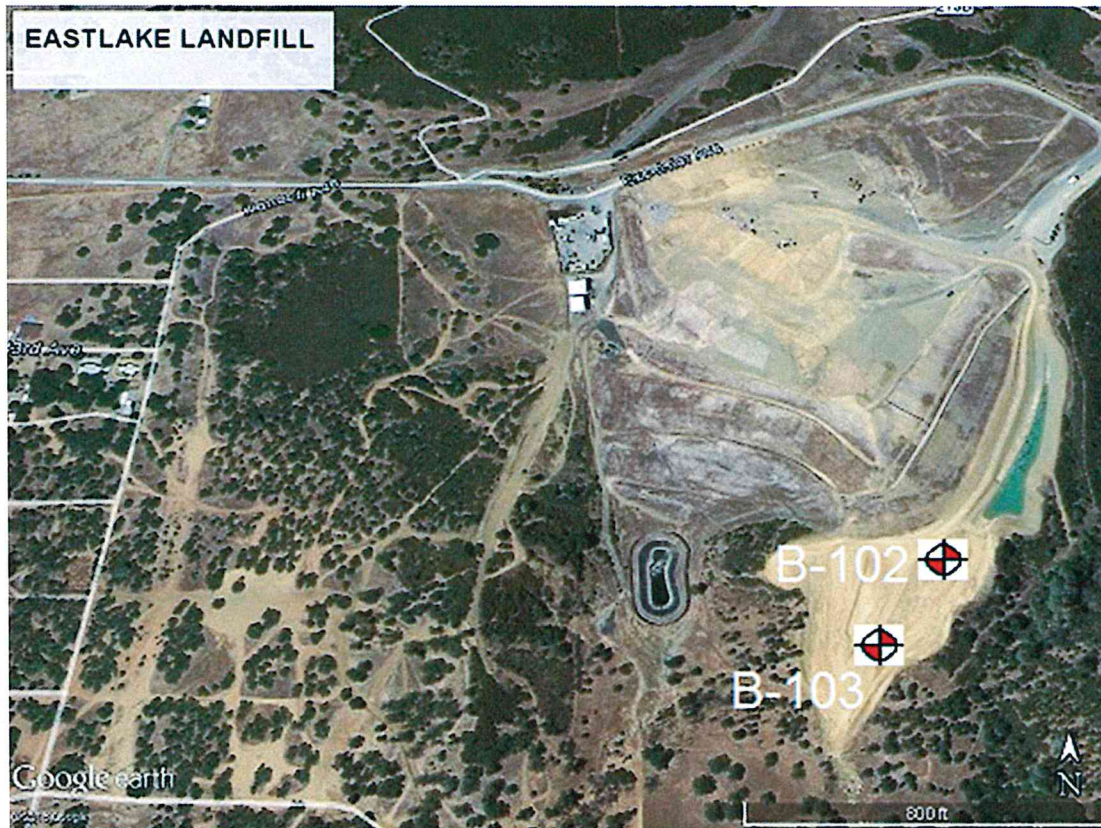


Figure 1: Borehole Location Map

6.0 RESULTS

The results of the BGL survey conducted in boreholes B-102 and B-103 are described in the following sections.

6.1 BORHOLE B-102

The results of the NG and EMI surveys conducted in B-102 are illustrated by the Log Summary Plot shown on Plate 1. This plate contains, from left to right, the following four columns of information:

Column 1 - A graph depicting the variation in NG (red line) and EMI (green line) versus depth according to the scales shown at the head of the column. The NG graph is in counts per second converted to American Petroleum Institute (API) units using a field standard. The EMI graph is in units of electrical conductivity (mS/m).

Column 2 – An unwrapped and un-interpreted combination OPTV and BHTV image that is provided for comparison purposes.

Column 3 – The depth scale used for all columns of data (in feet bgs).

Column 4 – A graph showing EMI (solid black line) versus depth in units of electrical resistivity (Ohm-m) according to the scale shown at the head of the column. This graph uses a larger horizontal scale than the electrical conductivity graph in Column 1 in order to show more detail.

The results of the borehole televiewer survey are illustrated in more detail in Appendix B. The images and graphs contained in this appendix also depict the results of the BC survey, the results of the televiewer fracture analysis and a depiction of the borehole inclination and drift. Explanations of these images and graphs are provided Appendix A, Section 4.4. The borehole discontinuities identified by the televiewer survey are listed in Table 2 at the end of Appendix A.

6.2 BOREHOLE B-103

The results of the NG, EMI and SBL surveys conducted in B-103 are illustrated by the Log Summary Plot shown on Plate 2. This plate contains, from left to right, the following five columns of information:

Column 1 - A graph depicting the variation in NG (red line) and EMI (green line) versus depth according to the scales shown at the head of the column. The NG graph is in counts per second converted to American Petroleum Institute (API) units using a field standard. The EMI graph is in units of electrical conductivity (mS/m).

Column 2 – An unwrapped and uninterrupted BHTV image that is provided for comparison purposes.

Column 3 – The depth scale used for all columns of data (in feet bgs).

Column 4 – A graph depicting the variation in P-wave interval velocity (V_p) versus depth according to the scale shown at the top of the graph.

Column 5 – A graph showing EMI (solid black line) versus depth in units of electrical resistivity (Ohm-m) according to the scale shown at the head of the column. This graph uses a larger horizontal scale than the electrical conductivity graph in Column 1 in order to show more detail.

More detailed results of the SBL survey are listed in Appendix A, Section 3.4, Table 1. This table lists not only Vp, as shown on Plate 2, but also the S-wave velocities (Vs) measured by the SBL survey.

The results of the borehole televiewer survey are illustrated in more detail in Appendix B. The images and graphs contained in this appendix also depict the results of the BC survey, the results of the televiewer fracture analysis and a depiction of the borehole inclination and drift. Explanations of these images and graphs are provided in Appendix A, Section 4.4. The borehole discontinuities identified by the televiewer survey are listed in Table 3 at the end of Appendix A.

Given the number of discontinuities identified by our fracture analysis we also computed a pole projection as shown on Plate 3. This plate contains a stereo-net that illustrates the distribution of discontinuities with regard to their dip magnitude and dip direction. A condensed version of the Dips Plot contained in Appendix B is included to the left of the stereo-net for comparison purposes.

7.0 DISCUSSION

7.1 BOREHOLE B-102

The televiewer images shown on the Log Summary Plat (Plate 1) indicate a very fine grained rock that is moderately fractured to massive. The natural gamma log shows slight variation in gamma intensity versus depth, ranging from 30 to 40 API units. This magnitude gamma intensity along with the fine grained texture noted on the televiewer logs indicate the lithology is a fine grain silty sandstone. The EMI electrical resistivity values range from 7 to 12 Ohm-m below 18-ft bgs. This range of electrical resistivity is consistent with silty sandstone. The resistivity values above 18-ft bgs increase dramatically. We do not think this increase in resistivity is related to lithologic change but rather as a response to the occurrence of open, near vertical fractures from 9- to 14-ft bgs. These fractures create air-filled voids or permeability that drive the resistivity higher.

7.2 BOREHOLE B-103

7.2.1 Summary Log Plot

The BHTV image included on Plate 2 indicates a bedded (possibly cross-bedded), fine grained rock that is moderate to little fractured to massive. In general, the natural gamma log shows slight gamma intensity variation with depth ranging in intensity from 30 to 40 API units. Electrical resistivities measured at depths of 12- to 64-ft bgs range between 10 and 20 Ohm-m. These magnitude gamma intensities and resistivities, along with the fine grain texture noted on the televiewer logs, suggest that the lithology consists of a fine grain silty sandstone. Exceptions to this generalization are the high gamma peak at 12.5-ft bgs and the high resistivity log excursion beginning below 64-ft that peaks at 55 Ohm-m near 70-ft bgs. The gamma high is probably caused by a more shaley sandstone inter-bed. The high resistivity probably indicates that the bedrock is becoming more indurated, massive with little or no weathering with increased depth. The BHTV log correlates to this interpretation as the image of borehole are shown to be hard (highly reflective) with no discontinuities (fractures) present.

The P-wave velocities depicted in the Summary Log Plot have an average value of about 6,000 feet per second (fps) in the depth range of 8- to 49-ft bgs. However, below 49-ft Vp increases gradually, to a value of 7,000-fps at 56-ft, and then rapidly reaching a value of 9,000-fps at 60-ft. The Vp inflection point at 56-ft bgs is interpreted as the boundary between moderately weathered-fractured bedrock above to little weathered, less fractured bedrock below.

7.2.2 Televiewer Interpretation

The discontinuities we identified on the televiewer images have been classified as major and minor fractures/joints and bedding. However, the dominate discontinuity feature appears to be geologic bedding. The bedding attitudes control the distribution of the subsurface lithology. In order to determine an average trend in the bedding dip direction and dip angle, we used the computer program WELLCAD Version 5.1 to create a Pole Projection on a stereo-net diagram, as shown on Plate 3. This diagram shows that most of the poles (dips) plot in the southwest quadrant. A center point within the highest closed contour of pole density (shaded dark brown) indicates the average bedding dips 37° from horizontal along a bearing of N227°.

8.0 STANDARD CARE AND WARRANTY

The scope of NORCAL's services for this project consisted of using the downhole geophysical techniques to identify lithology, map bedrock discontinuities and measure P-wave velocities. The accuracy of our findings is subject to specific site conditions and limitations inherent to the

SHN Consulting Engineers & Geologists
February 19, 2018
Page 7



techniques used. We performed our services in a manner consistent with the standard of care ordinarily exercised by members of the profession currently employing similar methods. No warranty, with respect to the performance of services or products delivered under this agreement, expressed or implied, is made by NORCAL.

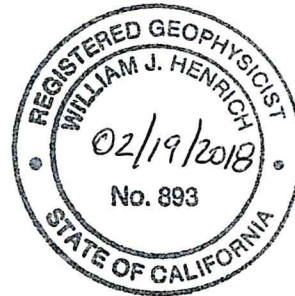
We appreciate the opportunity to provide our services to SHN for this investigation. Should you have questions or require additional geophysical services, please feel free to call.

Yours very truly,

NORCAL Geophysical Consultants, Inc.

A handwritten signature in black ink, appearing to read "William J. Henrich", is written over the printed name.

William J. Henrich
Professional Geophysicist PGp-893

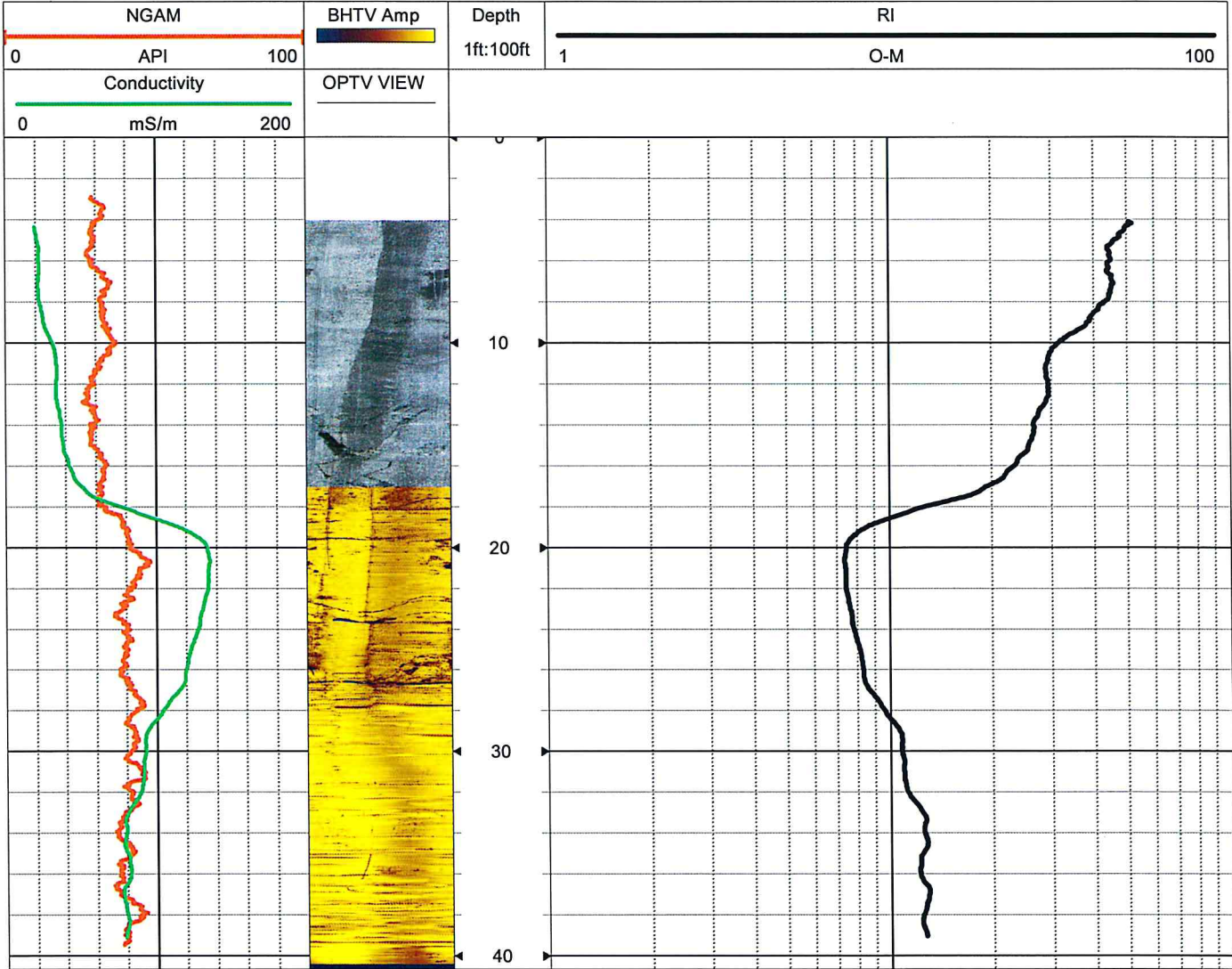


WJH/WEB/tt

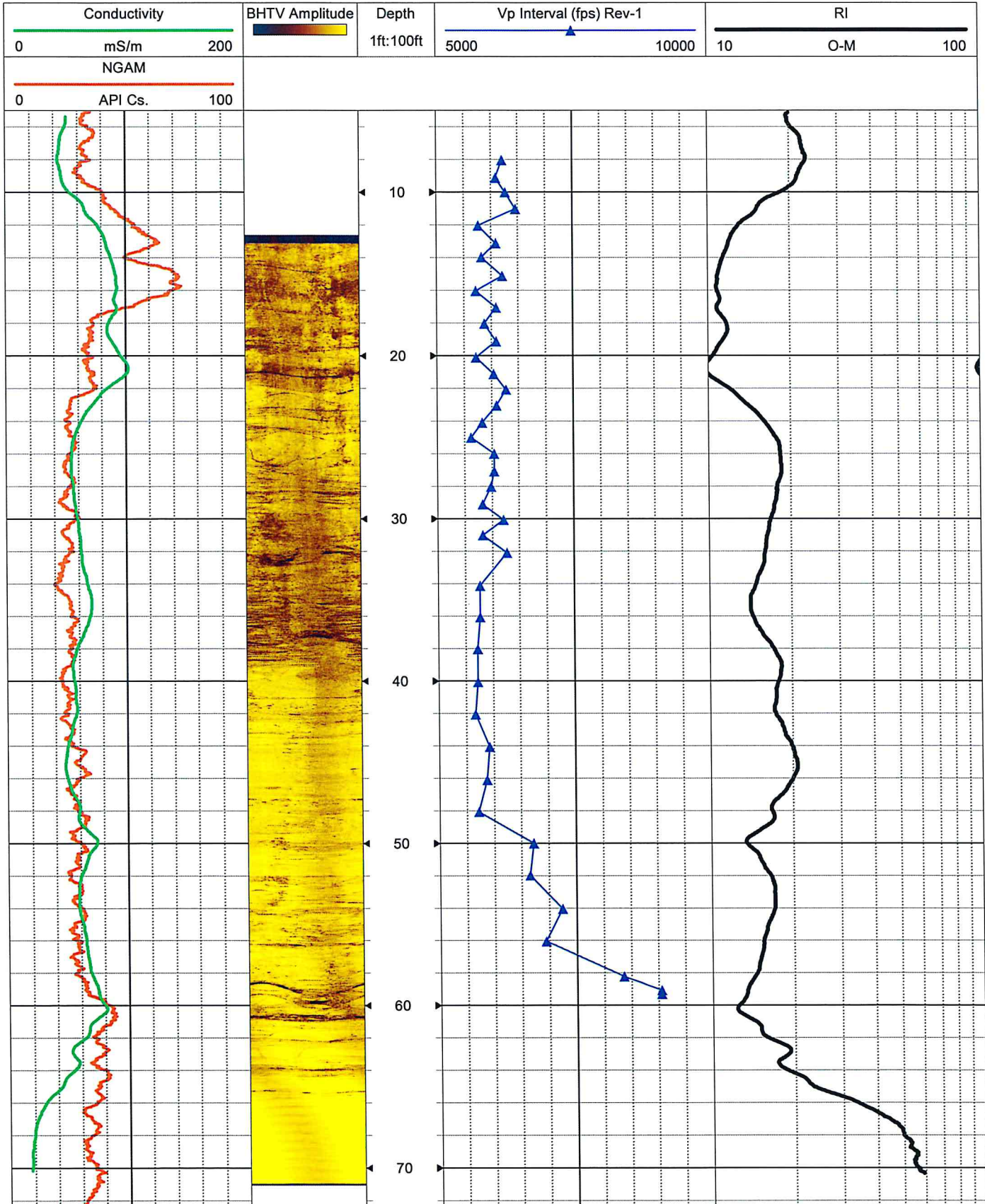
Enclosures: Plates 1-3
Appendices A & B

 <p>NORCAL NORCAL GEOPHYSICAL CONSULTANTS, INC.</p>	PLATE 1	COMPANY: SHN WELL ID: B-102 FIELD: EASTLAKE LANDFILL COUNTY: LAKE	DATE: DEC. 21, 2017 CASING: PVC to 3-ft bgs JOB NO. NS175076 STATE: CA
	LOG SUMMARY PLOT		

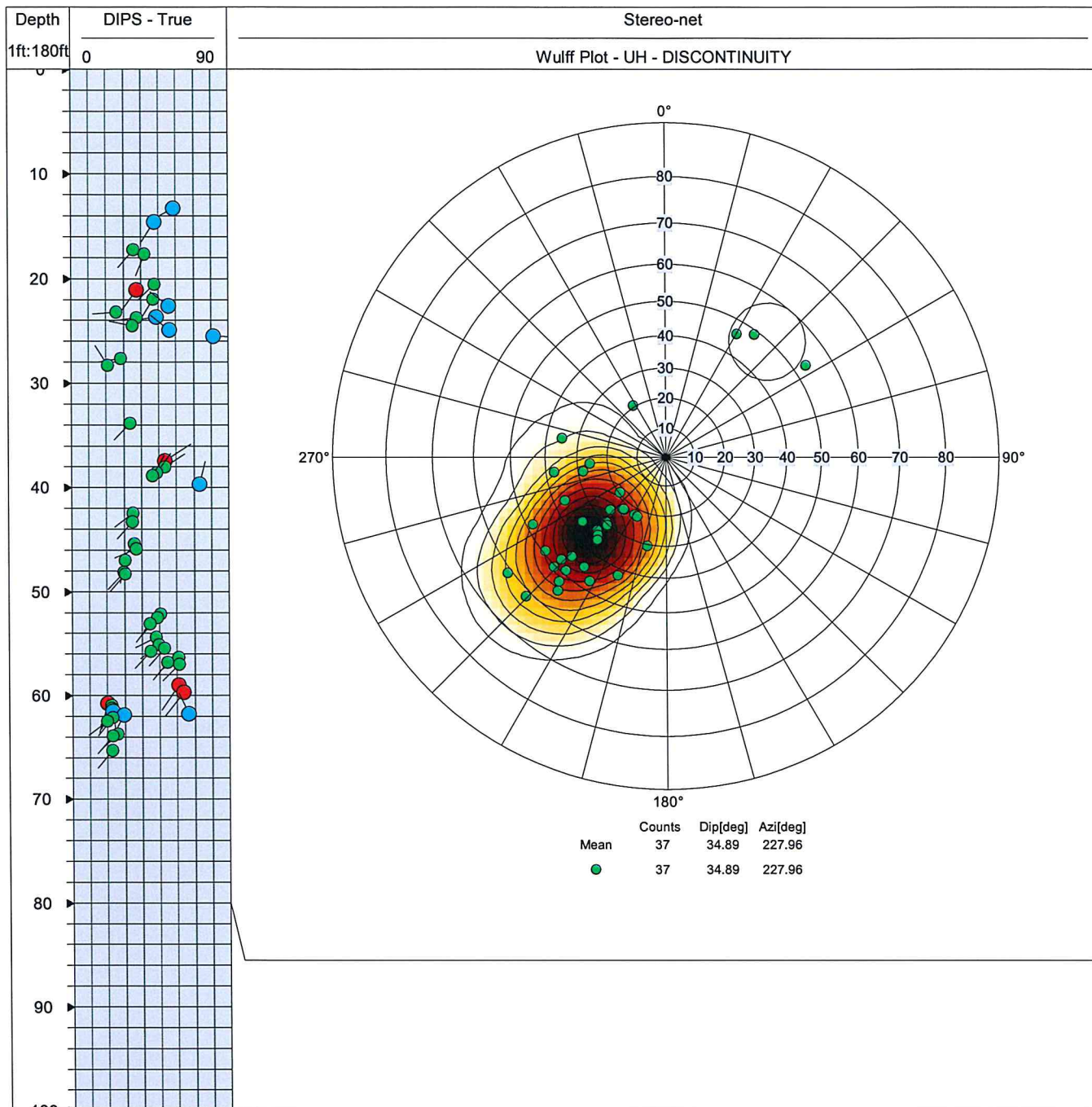
NOTES: Water level at 17-ft bgs during data acquisition; falling at ~ 5-ft per hour



NOTES:



NOTES: Bedding Dips plotted on the Projection



Appendix A
BOREHOLE GEOPHYSICAL LOGGING

APPENDIX A

BOREHOLE GEOPHYSICAL LOGGING

Boreholes B-102 and B-103 were logged using the Borehole Caliper, Natural Gamma, Electromagnetic Induction, Suspension Borehole Logging and Acoustic Borehole Televier methods. The instrumentation used to conduct these surveys is outlined below. Descriptions of the methodology, data acquisition and data analysis procedures and, in some cases, the results and interpretation for each technique are provided in Sections 1 – 4.

NORCAL conducted geophysical borehole logging using a digital **MICROLOGGER2** System manufactured by **Robertson Geologging, Ltd.** This system consisted of the following components:

- Control Console
- Computer
- Motorized Cable Winch
- Borehole Caliper Tool
- Single Spaced Induction Conductivity Tool
- Suspension Borehole Logger
- Optical televierer (OPTV)
- Acoustic Televierer (BHTV)

1.0 BOREHOLE CALIPER SURVEY

1.1 METHODOLOGY

The borehole caliper (BC) provides a direct measurement of borehole diameter and is used to determine potential hazards in the borehole due to caving or bridging. We typically conduct a BC survey in every borehole prior to committing more expensive tools to the open hole. The caliper is a mechanical tool consisting of three spring loaded arms that, when deployed, press against the borehole wall. Variations in the average arm extension, as registered on a potentiometer, provides an indication of borehole diameter once the tool has been calibrated.

1.2 DATA ACQUISITION

Prior to conducting the Borehole Caliper (BC) survey in each borehole, the tool was calibrated using a set of rings of known diameter ranging from 4.0 to 8.0 inches. Following calibration, the tool was lowered to the bottom of the borehole where the arms were extended until making contact with the borehole wall. The tool was then raised upward in the borehole at a rate of about 10 feet per minute. This resulted in a digital sampling interval of 0.05 feet.

1.3 DATA ANALYSIS

The BC data were incorporated into the computer program WELLCAD Version 5.1 published by ALT, Luxemburg. We then used this program to electronically merge the BC log traces with the NG and EMI log traces (Section 2.0) and the televiewer images (Section 4.0) to form the Log Summary Plots shown Plates 1 and 2. The interpretation of these plots is discussed in the main body of the report.

2.0 NATURAL GAMMA AND ELECTROMAGNETIC INDUCTION

2.1 METHODOLOGY

Natural gamma (NG) logging records the amount of gamma radiation emitted by naturally occurring isotopes found in unconsolidated alluvial and bedrock formations. These isotopes are primarily Potassium-40 (K) and decay series products of thorium (Th) and uranium (U). Relatively high gamma intensities typically occur in shale (mudstone) and alluvial clay deposits because these geologic units contain potassium bearing clay minerals and very small concentrations (in the ppm range) of uranium and thorium ions that are electrically bound on the clay mineral lattice. Relative low gamma intensities are associated with well-sorted unconsolidated coarse sand and gravel deposits or consolidated sandstones. This assumes coarse-grain sediments and the sandstone matrix consist primarily of quartz with only very small percentages of gamma-emitting feldspar. The natural gamma intensity is measured in counts per second and converted to American Petroleum Institute (API) units using a field standard.

Electromagnetic Induction (EMI) is a means of measuring the electrical conductivity of a volume of earth material without direct contact through the electromagnetic induction method. Electrically energized transmitter coils in the probe produces a primary electromagnetic field, which induces an alternating voltage ground loop flow in adjacent geologic formations. The ground loop creates a secondary electromagnetic field that is detected by a receiver coil. The measured strength of the secondary field is proportional to the electrical conductivity of the formation. A major advantage of the EMI method is that it does not require direct contact with the formation. Consequently, the electrical conductivity data can be collected in dry, open borings or in non-metallic (e.g. PVC) cased wells. Electrical conductivity is a function of grain

size, consolidation, effective porosity, pore water salinity, and percent water saturation. In general, fine-grained, unconsolidated silt-clay sediments or consolidated shale and mudstones produce high electrical conductivities, e.g. >200 mS/m. Conversely, coarser grain alluvial sand, gravels, or consolidated sandstone bedrock produce relatively low conductivity values, e.g. < 20 mS/m.

2.2 DATA ACQUISITION

The Natural Gamma (NG) and Electromagnetic Induction (EMI) tools are housed in the same probe. Prior to logging the EMI component of the probe was calibrated with a formation conductivity simulator coil. This device uses calibration ranges of 0, 105 and 415 mS/m. The NG component does not require calibration. Two logging runs were made with the combined tool in each borehole; one to measure NG response only and a second to measure both NG and EMI simultaneously. For both runs, the probe was lowered to the bottom of the open borehole then raised upward at a logging speed of 10 feet per minute. This resulted in the logging response being digitally sampled (recorded) at 0.05 foot intervals. Having at least two logging runs in each borehole helped to demonstrate log consistency.

2.3 DATA ANALYSIS

The NG and EMI data were incorporated into the computer program WELLCAD Version 5.1 published by ALT, Luxemburg. We then used this program to electronically merge the NG and EMI log traces with the BC log trace (Section 1.0) and the televiewer images (Section 4.0) to form the Log Summary Plots shown on Plates 1 and 2. The EMI data are displayed in units of electrical conductivity (mS/m) on the left side of the plot, and in the inverse units of electrical resistivity (O-M) on the right side. The resistivity scale is much larger than the conductivity scale in order to depict subtle variations in resistivity. The interpretation of the Log Summary Plots is discussed in the main body of the report.

3.0 SUSPENSION BOREHOLE LOGGER

3.1 METHODOLOGY

A Suspension Borehole Logger (SBL) is a tool that is used to measure compressional (P-) and shear (S-) wave velocities in an open borehole. We conduct SBL surveys using a Robertson Geologging, Ltd. digital suspension logging system. A schematic diagram depicting the probe configuration and equipment is shown in Figure 1. The suspension logging tool is equipped with a dipole seismic energy source located near the bottom of the probe and a pair of detectors (receivers) designated as R1 and R2, located within the middle to the upper sections. The distance from the energy source to the closest receiver is 10.3 feet (3.15meters) when assembled with a detachable 2-meter isolation tube. The in-line distance between the receiver pair is 3.28-feet (1.0 meter). Each receiver contains one horizontal and one vertical oriented element. The horizontal elements preferentially record horizontally polarized S-wave motion and the vertical receiver elements preferentially record first arriving P-wave energy.

When assembled with a 2-meter isolation tube, the suspension logging tool is approximately 23-ft long. By definition, the depth reference point of the tool is half-way between the two receivers. Since this point is approximately 15-ft from the probe tip, the maximum depth of an SBL survey, given a non-sloughing borehole, will always be reported as 15 feet less than the total depth of the borehole. In operation, the probe is centralized in the borehole with flexible rubber rings positioned just below the source and just above the receiver section. This is necessary in order to maintain a gap between the probe housing and borehole wall.

Suspension borehole logging data are collected at discrete depths in the fluid-filled portion of the borehole. At each measurement depth, the energy source is activated via commands from the surface control console. This activation causes a metal solenoid (hammer) to horizontally strike the inner probe housing (anvil). This energy propagates through the fluid to the borehole wall which produces a seismic "flexure" wave in the adjacent formation. As this wave propagates radially into the formation a physical interaction between the seismic wave and the borehole wall creates tube waves together with refracted P-waves that travel up the borehole to the two receivers.

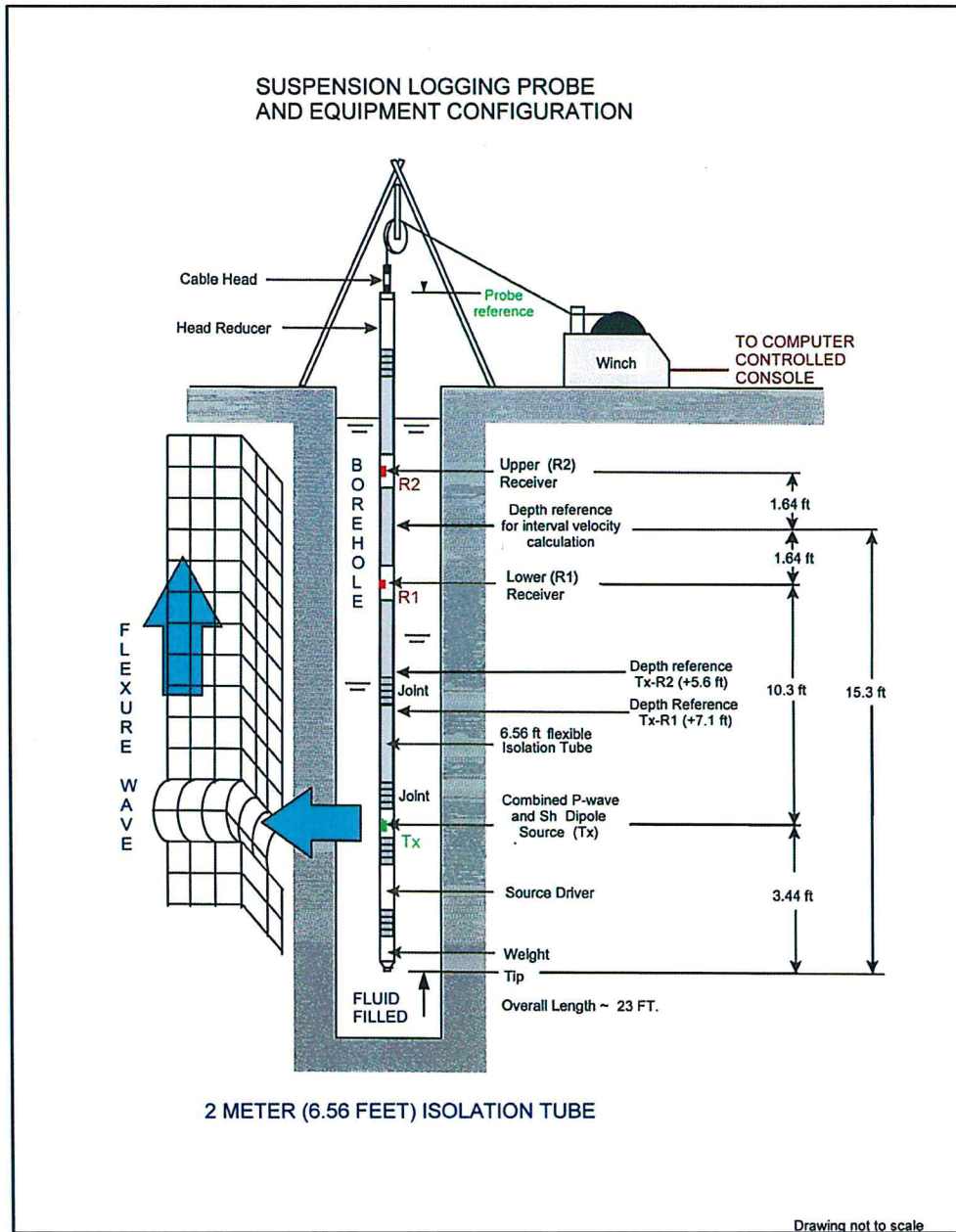


Figure 1: Suspension Borehole Logger schematic diagram

3.2 DATA ACQUISITION

The suspension borehole logging survey (SBL) was conducted in Borehole B-103 only. Although the tool measures both compressional (P-) and shear (S-) wave velocities, in this case we used it solely for the purpose of measuring P-wave velocities (V_p). This was done in order to provide information on subsurface velocity contrasts in advance of a seismic refraction survey.

We measured P- and S-wave velocities at stationary depth positions distributed at 0.5 to 2.0-foot intervals throughout the accessible depth range of the borehole. The survey began with the depth reference point of the probe positioned near the bottom of the borehole, at a depth of approximately 60-ft below ground surface (bgs). The survey then proceeded upward to a depth of 8-ft bgs. At each measurement station, we cycled the energy source to fire 1 to 2 times in succession into each of the receiver elements. This cycling algebraically summed (stacked) the seismic energy resulting in an enhanced signal-to-noise ratio. We recorded S-wave velocities by applying a 1.2 KHz low pass filter to the signals detected by the horizontal receiver elements. This filtering reduces high frequency interference from the onset of earlier arriving P-wave energy on the S-wave channels. We recorded P-wave velocities using a 20 KHz low pass filter.

3.3 DATA ANALYSIS

Suspension P- and S-wave velocities were calculated with the interpretation computer software programs PSLogger Application Version 1.121 and PSLOG Analysis Version 1.0.001. Both programs are published by Robertson Geologging, Ltd. (2009). Sample suspension logger seismic records from Borehole B-103 are presented in Figures 2 and 3. These samples were recorded at depths of 22- and 58-ft below ground surface (bgs), respectively. Individual records display six seismic wave-traces. The upper four traces were detected by the horizontal receiver elements and are used to identify S-wave arrivals. These traces are labeled according to the wave type (s=shear), the direction of the hammer against the anvil (l=left and r=right) and the relative distance from the source (n=near and f=far). For example, the top wave trace is labeled "srf". This indicates that it was recorded to identify S-waves using a right strike at the far receiver. The seismic S-wave traces produced by a right hand strike of the source (Cycle 1) are colored red for both the near and far receivers. The seismic S-wave traces produced by a left hand strike of the source (Cycle 2) are colored green for both the near and far receivers.

The lower two traces were detected by the vertical receiver elements and are used to identify P-wave arrivals. These traces are labeled according to the wave type (p=primary) and the relative distance from the source (n=near and f=far). For example, the bottom most wave trace is labeled "pn" because it was recorded to identify P-waves by the near receiver. These seismic wave traces are produced during Cycle 3 and are colored blue. Since they were detected by the vertical elements in the receivers, the direction of impact is inconsequential and is not addressed by separate waveforms. Note that the time window S-wave records in Figure 2 (0 to

14K microseconds) is four times larger than the time window for the P-wave records (0 to 3.5K microseconds). Suspension records that appeared ambiguous or lacked useable S-wave information were discarded from the final presentation of velocities.

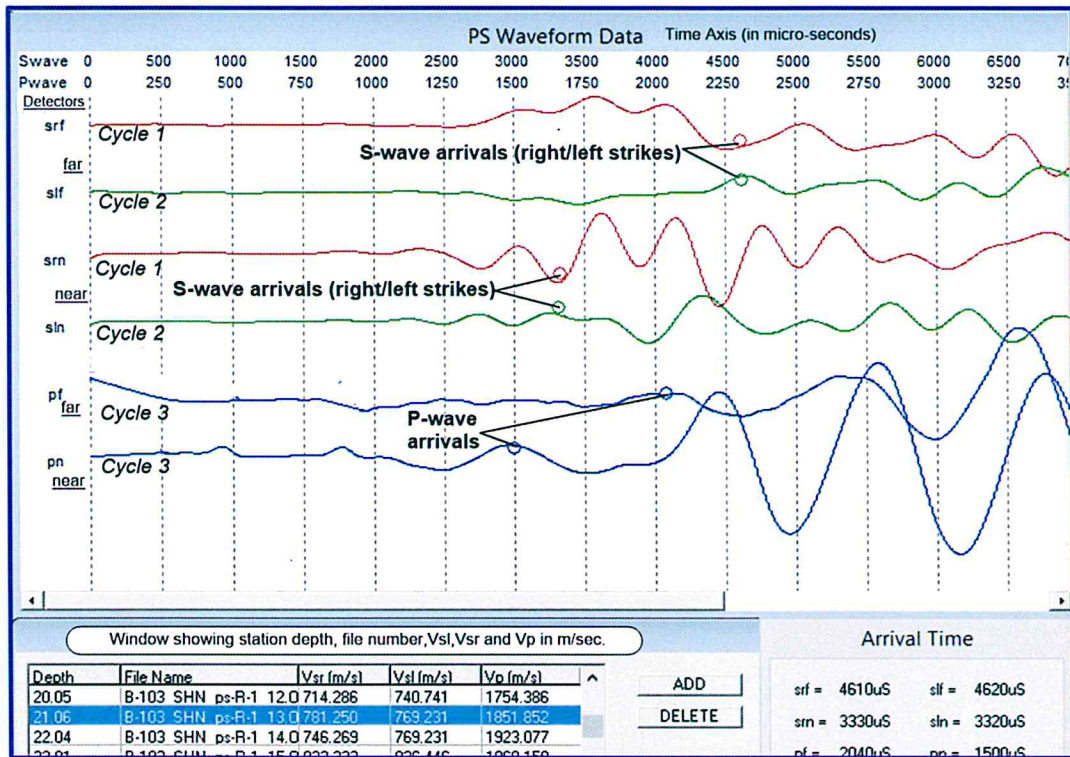


Figure 2: Sample seismic record from B-103 at depth 21-ft bgs

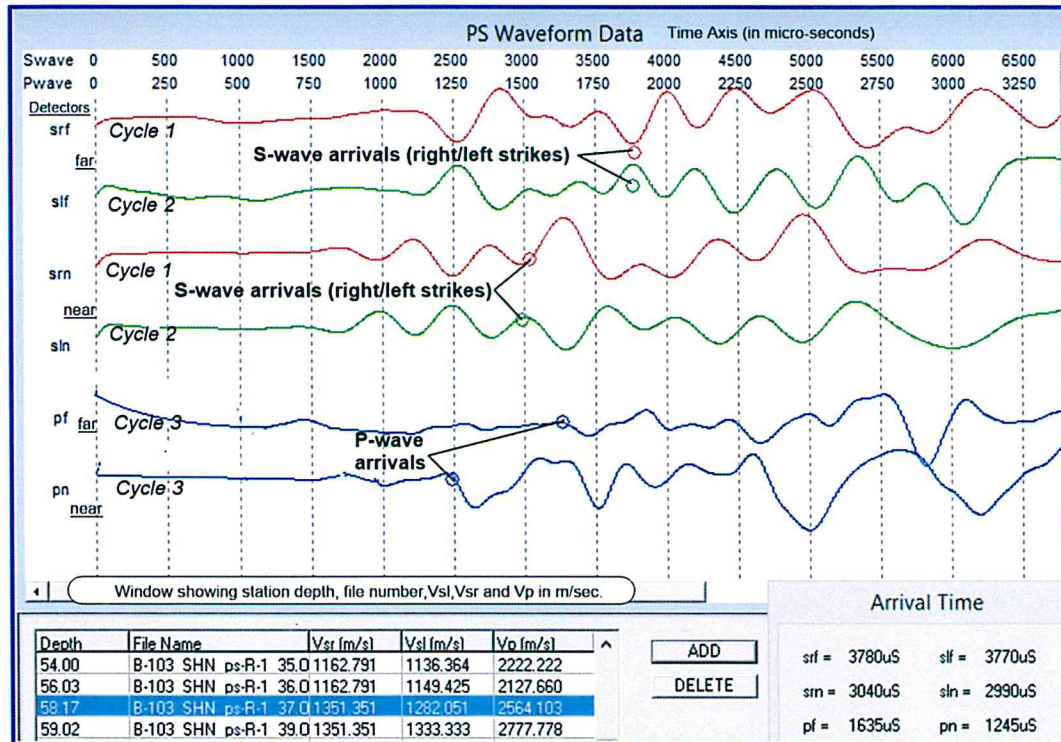


Figure 3: Sample seismic record from B-103 at depth 58-ft bgs

3.3.1 S-Wave Arrivals

On the seismic records shown in Figures 2 and 3, the red traces (Cycle 1) were created by right anvil strikes or impacts and the green traces (Cycle 2) were created by left anvil strikes. Pairing the traces produced by opposite directions of impact reveals a phase reversal that is associated with the onset (arrival) of S-wave energy. However, because there can be slight discrepancies in timing between Cycle 1 and Cycle 2, the reversal point may not occur at the same exact time on both traces. Therefore, the onset of S-wave energy is further defined as the point where there is also a significant increase in amplitude within the phase reversal time window. These arrival times are depicted by open dots on the upper four wave traces.

3.3.2 P-Wave Arrivals

P-wave arrivals are identified as the point where the wave traces produced by Cycle 3 (blue) change from straight lines to sinusoidal wave forms. These points, referred to as a “first breaks” are represented by blue circles on the lower two wave traces.

3.3.3 Seismic Velocity Calculations

Seismic wave velocities (V) are calculated by dividing the distance (X) from the source to a given receiver by the time required (T) for the seismic wave to reach that receiver. Hence, $V = X/T$. This is referred to as a direct path seismic velocity. However, velocities can also be calculated by dividing the distance between the two receivers (R1 and R2) by the difference in travel time to those receivers (T2-T1). This is considered an interval velocity. For example:

$$V (R2-R1) = (XR2-XR1) / (TR2-TR1)$$

Where XR1 and TR1 are the distance and travel time to the first receiver (R1); and XR2 and TR2 are the distance and time to the second receiver (R2). The separation between receivers is one-meter.

3.3.4 Interval Seismic Velocities

We used the travel times measured in Borehole B-103 to compute four interval velocities; three S-wave (Vs) and one P-wave (Vp). The interval Vs were computed using the Cycle 1 (VsRight) and Cycle 2 (VsLeft) travel times and their average. The interval Vp were computed using the Cycle 3 travel times. All station depths and velocities are listed in Table 1. The velocities are listed in both metric (meters, meters per second) and Imperial (feet, feet per second) units. As indicated in the Data Acquisition section we collected several PS-velocity files and thus velocity profiles with overlap. As a result of this data density, the station spacing along the upper portions of the finalized velocity profile are closely spaced and in some cases show station duplication. In order to integrate the closely spaced data and smooth the velocity distribution, we applied a 3-point running average to both Vs and Vp. The resulting smoothed values are presented in the two far right columns of the following table. These values represent our interpretation of the Vs-Vp distribution with depth. They are shaded blue in the table and are graphed on Plate 1 in the main body of the report. We based our interpretation on the interval velocities because they are the least susceptible to variations in triggering and/or coupling errors. The depths of the measurements are based on a probe reference point that is half-way between the near and far receivers.

3.4 RESULTS

The results of the SBL survey are illustrated by the blue triangles plotted in the Vp Interval versus Depth graph included on the Log Summary Plot, Plate 2. The results are also presented in Table 1. The depths listed in the table are below ground surface (bgs) relative to a point on the probe that is half-way between the two detectors (Figure 1). The velocities listed in the table are interval velocities as described in Section 3.3.4.

TABLE 1. B-103 P- and S-WAVE VELOCITY TABLE

Depth (ft)	Vs (fps)	Vp (fps)
8.0	1919	6211
9.1	2204	6095
10.0	2136	6271
11.0	2045	6457
12.0	2090	5772
13.1	2273	6095
14.0	1942	5823
15.1	2370	6211
16.0	2187	5721
17.0	2516	6095
18.0	2534	5875
19.1	2319	6095
20.1	2387	5721
21.1	2543	6039
22.0	2486	6271
23.0	2723	6095
24.0	2534	5823
25.0	2594	5622
26.0	2430	6039
27.0	2335	6039
28.0	2327	5983
29.1	3528	5823
30.0	2476	6211
31.0	2287	5823
32.1	2311	6271
34.1	2232	5772
36.0	2458	5772

Depth (ft)	Vs (fps)	Vp (fps)
38.0	2232	5721
40.0	2574	5721
42.0	2232	5671
44.0	2026	5929
46.1	2524	5875
48.0	2486	5721
50.0	3886	6724
52.0	3510	6655
54.0	3772	7246
56.0	3793	6938
58.2	4320	8361
59.0	4404	9058
59.3	4557	9058

4.0 BOREHOLE TELEVIEWER SURVEY

4.1 METHODOLOGY

Borehole Televiewers are downhole tools that are used to produce digital radial images of the interior of a borehole. The images are composited sequentially using computer software to produce continuous color images. These images are like unfolded, or unwrapped, cylinders displayed on a two-dimensional surface. The “unwrapped” radial images are referenced to magnetic north by an on-board magnetic compass. In addition, an on-board three-axis magnetic inclinometer determines the inclination and azimuth of the borehole versus depth.

Televiewer images can be used to detect bedrock discontinuities (joints, fractures, bedding planes, geologic contacts, etc.) borehole wall textures, and other descriptive geologic information. Interpretable discontinuities appear as thin sinusoidal forms that stretch across the image. Interactively fitting lines to these sinusoids provides data that the computer software uses to determine the orientation and dip of the discontinuities. The midpoint, or half amplitude, of a sinusoid is taken as the depth of the discontinuity.

There are two types of televiewers; optical and acoustic. Optical televiewers (OPTV) use a digital optical sensor to produce radial images to a vertical resolution as fine as 0.004 feet and a radial resolution to 720 pixels. However, they can only be used in dry holes or in holes filled with water of sufficient clarity to create an interpretable high resolution image. Acoustic televiewers (BHTV) require a water column to act as a medium for the transmission and reception of

acoustic signals. The water does not have to be optically clear. In operation the BHTV transmits an ultrasonic signal into the borehole fluid and detects ultrasonic energy that is reflected from the borehole wall. Sidewall borehole images are created by measuring variations in the two-way travel time of the ultrasonic pulses as well as variations in the amplitude of the reflected signals

4.2 DATA ACQUISITION

Prior to the survey it was postulated that acoustic televiewer methods might resolve minor fractures at this location more confidently than optical methods. Therefore, we logged both boreholes using the BHTV tool. Prior to logging, each borehole was filled with water to provide a transmission medium for the BHTV survey. In addition, we checked the correct operation of the tools onboard compass. This involved comparing bearing directions taken with the onboard compass against readings taken with a hand held Brunton Compass. Variations of no greater than 1- to 2-degrees in azimuth between the tool display and the Brunton Compass confirms that the tools compass is operating satisfactorily.

Our operational procedure was to lower the tool to the bottom of the borehole and then acquire data while raising the tool upward at a constant rate of 4.5-ft per minute. This resulted in data sampling intervals of between 0.004 and 0.006 feet, respectively.

We conducted two BHTV runs of in each borehole. This was done in order to demonstrate the repeatability of the orientation of common borehole features. Additionally, the second televiewer run was recorded with changes in signal gain in order to optimize the image quality.

During the course of the BHTV survey, we discovered that the fluid level in B-102 had dropped to a depth of approximately 17-ft bgs. Since this represented a substantial percentage of the open borehole that could not be logged with the BHTV, we substituted an OPTV survey in the air-filled portion of the hole. The same calibration, operational checks and acquisition procedures were used with the OPTV survey that we had applied to the BHTV logging.

4.3 DATA ANALYSIS

We used the computer program *WELLCAD* (Version 5.1, ALT, and Luxemburg) to produce televiewer image plots and to electronically merge them with the BC, BG, EMI traces to form the Log Summary Plots shown on Plates 1 and 2. We also used the software to calculate orientations of interpreted discontinuities (e.g. fractures, joints, bedding). Corrections for the magnetic declination in the survey area required adding 13.5 degrees to the magnetic compass bearings in order to orient the borehole images to true north (NOAA, Magnetic Declination Calculator, 2017). Since borehole diameter is a major reduction parameter in determining dip magnitude, we input caliper log measurements. Discontinuities analysis was performed interactively on sections of the unwrapped televiewer images as viewed on a computer monitor.

An interpretable discontinuity on a two-dimensional unwrapped borehole televiewer log appears as a recognizable sinusoidal trace that usually extends across the full width of the borehole image. An example of a discontinuity on a BHTV image is shown in Figure 4. The sinusoidal shape is a manifestation of a planar discontinuity intercepting a three-dimensional cylindrical borehole. Planar discontinuities can be geologic features that include discrete fractures or joints, bedding planes and planar intrusions such as veins and geologic contacts. Identified discontinuity traces on the image logs are fitted with a bendable sinusoid that overlies the trend of the discontinuity trace. *WELLCAD* then calculates a plane that represents the orientation of the discontinuity in terms of dip direction and dip magnitude based on the position of the sinusoid overlay. The process is repeated for every significant discontinuity until the entire borehole is interpreted. At this stage, apparent dip direction and dip magnitude of the discontinuities are converted to true geographic dip azimuth and dip magnitude by factoring the borehole tilt (inclination) and azimuth at the depth of the discontinuity.

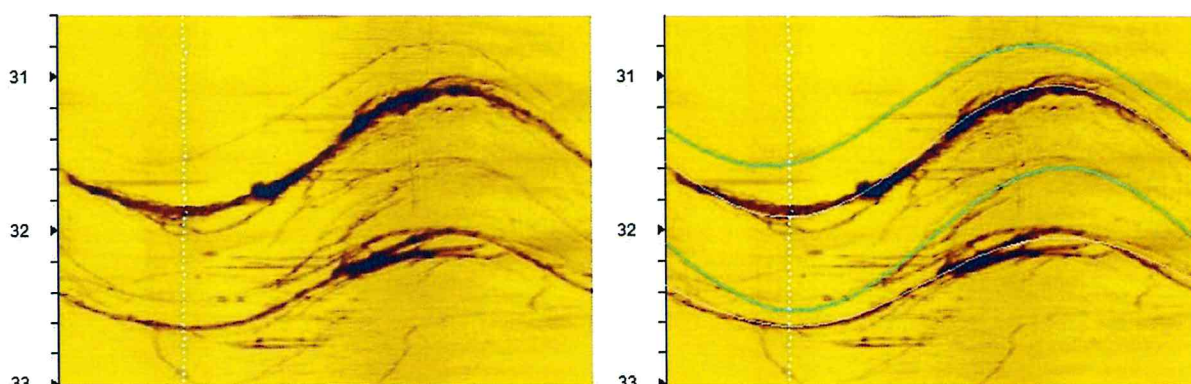


Figure 4: A sample BHTV section showing observable discontinuity traces (left) versus the same image (right) with the addition of interpreted sinusoidal overlays (green and tan colored traces).

Based on observations and our own experience identifying planar features on televiewer images, we classified discontinuity features into four categories or classifications as follows:

- 1) "Major continuous fractures/joints". These have characteristics that are relatively wide (measureable $\gg 1\text{mm}$) apparent apertures, continuous sinusoidal traces across the circumference of the borehole wall and show relief/breakage along the borehole wall. This relief is usually shown as diameter enlargements on the caliper log. Some apertures were so wide that the region between lower and upper bounds of the features were hachured. The interpretation program treats these as one feature and provides a true thickness calculation in 1/10 inches.

2) "Minor fractures/joints, continuous or discontinuous". These features generally have thin ($< 1\text{mm}$) apparent apertures, sometimes shown as continuous traces or can be irregular and discontinuous especially when trace magnitude indicate high dip angles.

3) "Bedding". These features are closely spaced (a few tenths of a foot apart) discontinuities that tend to have the same dip angle and bearing direction. On a BHTV log, the bedding is distinguished by tonal changes from dark to bright yellow. Bedding traces are not manifested as relief changes to the borehole diameter. We found that bedding dip and direction in a single borehole was not constant. Whether these dip attitude variations are due to cross-bedding or due to fault movement must be verified by core observations.

We did not tabulate (interpret) cemented or highly discontinuous or fragmented fractures.

4.4 INTERPRETATION

The interpreted results of the BHTV/OPTV surveys conducted in B-102 and B-103 are illustrated as a series of graphical column plots presented in Appendix B. Each of these plots are several pages long, with header information presented at the top of the first page only. Each plot contains the following columns of information described, from left to right, as follows:

Column 1 - Depth

The depth axis indicates the relative vertical distance from the ground surface. Ground surface was set equal to zero feet. Depth values are positive and accumulate in the downward direction.

Column 2 – Televiewer Image

This is an unwrapped acoustic image representing the interior of the borehole wall, except in the upper 17 feet of B-102, which is optical. The images are oriented relative to true North as indicated by the azimuth information presented in the header where North, East, South and West correspond to 0° , 90° , 180° and 270° , respectively. The diameter of the borehole is indicated by the white dashed line superimposed on the image. Solid red or green lines superimposed on the images indicate those sinusoidal traces that, in our interpretation, represent significant discontinuities.

Column 3 - DIPS Plot

The Dips Plot indicates the dip of discontinuities and their direction of maximum dip. These parameters are indicated by small symbols called "tadpoles" which consist of a circle with a

straight line (tail) extending from it. The position of the tadpole indicates the degree of dip, from 0° on the left to 90° on the right, according to the scale shown at the top of the column. The direction that the tail is pointing indicates the direction of dip where straight up is true north and 90° to the right indicates due east. The color of the tadpole indicates the type of discontinuity. Red = Major fracture and joints; teal = Minor fractures and joints and green = bedding. The numerical values of dip azimuth and dip angle are also presented in Discontinuity tables (Section 4.5).

Column 4 - Core Plot

This plot is a graphic rendering of the OPTV or BHTV image into a 3-D core. This is basically what the televiewer image would look like if it was re-wrapped to form a cylinder where the vertical center line of the cylinder represents an azimuth written in the sub-header of the plot, the right edge represents 90° west of the azimuth; the left edge represents 90° south of the azimuth. Planes drawn through the interpreted discontinuities illustrate the dip angle and dip direction of the interpreted discontinuities.

Column 5 - Borehole Deviation

This plot indicates the azimuth and tilt of the borehole. The solid blue line represents the dip direction, from 0° to 360°, according to the header scale labeled “Azimuth”. The dotted green line represents the angle of the borehole from true vertical, from 0° to 90°, according to the header scale labeled “Tilt”. This scale ranges from 0° to 4°.







4.5 DISCONTINUITY TABLES

The dip azimuth and dip angle of all interpreted discontinuities from the televiewer analysis plots for boreholes B-102 and -103 are tabulated in the Discontinuity Tables provided in following section. The tables present five columns of data labeled from left to right as follows: Depth, Dip Azimuth, Dip Angle, Corrected Aperture and Discontinuity Classification. A brief description of the meaning of these terms is presented below.

- **Depth** – relates to the center of discontinuity’s sinusoid in feet (bgs).
- **Dip Azimuth** – dip direction of the discontinuity in degrees from true North.
- **Dip Angle** – inclination of the plane of the discontinuity in degrees from horizontal.
- **Corrected Aperture** – true thickness of fracture/joint corrected for dip measured in tenths of inches. In this survey, we used this processing facility to indicate the true thickness of weathered/altered fractures and joints.

- **Discontinuity Classification** – number designating classification type of fracture/joint and bedding (see Legend for explanation).

TABLE 2. BOREHOLE B-102 DISCONTINUITY TABLE

DISCONTINUITY LEGEND				
Code	Tadpole	Sine Wave		
1			"major" continuous fracture/joint	
2			"minor" continuous or diiscontinuous joint/fracture	
3			Bedding	

B-102 DISCONTNUITY TABLE				
Depth	Dip Azimuth	Dip Angle	Aperture or Thickness	Discontinuity Classification
ft	deg	deg	1/10 inches	(see Code under Legend)
6.89	268.69	32.73	nd	3
8.83	108.87	23.84	nd	2
9.16	118.92	57.24	nd	2
10.03	316.33	70.41	nd	2
10.72	290.55	54.54	nd	3
12.11	277.26	53.92	nd	3
13.34	126.59	64.99	nd	2
13.57	121.32	66.21	nd	2
14.37	135.19	78.25	9.3	1
16.68	261.11	60.74	nd	2
16.74	172.88	52.55	nd	2
17.81	165.51	49.42	nd	2
19.6	242.56	23.35	nd	2
20.2	39.47	63.87	nd	2
22.88	134.19	54.37	nd	2
23.28	130.72	78.39	nd	2
23.38	139	44.78	nd	1
26.63	254.67	21.62	nd	2
26.64	121.02	80.72	nd	2
31.28	262.27	42.48	nd	2

TABLE 3. DISCONTINUITY TABLE BOREHOLE B-103

B-103 DISCONTNUITY TABLE				
Depth	Dip Azimuth	Dip Angle	Aperture or Thickness	Discontinuity Classification
ft	deg	deg	1/10 inches	(see Code under Legend)
13.28	241.93	58.93	nd	2
14.6	213.99	47.66	nd	2
17.24	220.29	35.73	nd	3
17.65	202.31	42.02	nd	3
20.56	225.81	47.68	nd	3
21.11	216.15	37.63	nd	1
21.97	211.96	47.29	nd	3
22.6	307.72	56.16	nd	2
23.21	265.12	26.03	nd	3
23.67	262.3	49.02	nd	2
23.75	262.23	37.49	nd	3
24.5	280.57	35.23	nd	3
24.9	308.63	56.27	nd	2
25.49	91.53	81.56	nd	2
27.63	260.3	28.43	nd	3
28.29	327.96	20.89	nd	3
33.84	223.72	33.54	nd	3
37.43	57.18	53.45	9.43	1
38.03	56.75	53.49	nd	3
38.58	36.18	48.99	nd	3
38.88	30.2	46.43	nd	3
39.68	13.44	73.48	nd	2
42.46	232.63	35.15	nd	3
43.31	221.52	34.62	nd	3
45.4	219.82	35.79	nd	3
45.91	246.9	36.8	nd	3
47.03	192.4	30.46	nd	3
48.14	222.79	29.68	nd	3
48.32	221.15	30.34	nd	3
52.14	225.7	50.54	nd	3
52.48	221.6	49.05	nd	3
53.08	217.09	44.79	nd	3
54.37	243.25	48.3	nd	3
55.12	232.25	49.51	nd	3

B-103 DISCONTNUITY TABLE				
Depth	Dip Azimuth	Dip Angle	Aperture or Thickness	Discontinuity Classification
ft	deg	deg	1/10 inches	(see Code under Legend)
55.46	220.86	52.66	nd	3
55.73	223.63	44.83	nd	3
56.33	233.94	61.05	nd	3
56.8	219.24	54.7	nd	3
56.97	225.36	61.42	nd	3
58.99	214.74	61.1	nd	1
59.71	217.99	63.72	nd	1
60.75	196.57	20.08	18.32	1
60.93	209	22.29	nd	3
61.26	206.04	22.36	nd	3
61.56	171.78	22.89	nd	2
61.8	335.19	66.54	nd	2
61.9	208.96	29.47	nd	2
62.1	218.78	22.91	nd	3
62.49	232.81	19.81	nd	3
63.7	227.17	26.01	nd	3
63.9	220.38	23.16	nd	3
65.29	219.4	22.77	nd	3

NOTE: "nd" = NOT DETERMINED

Appendix B

BOREHOLE TELEVIEWER PLOTS

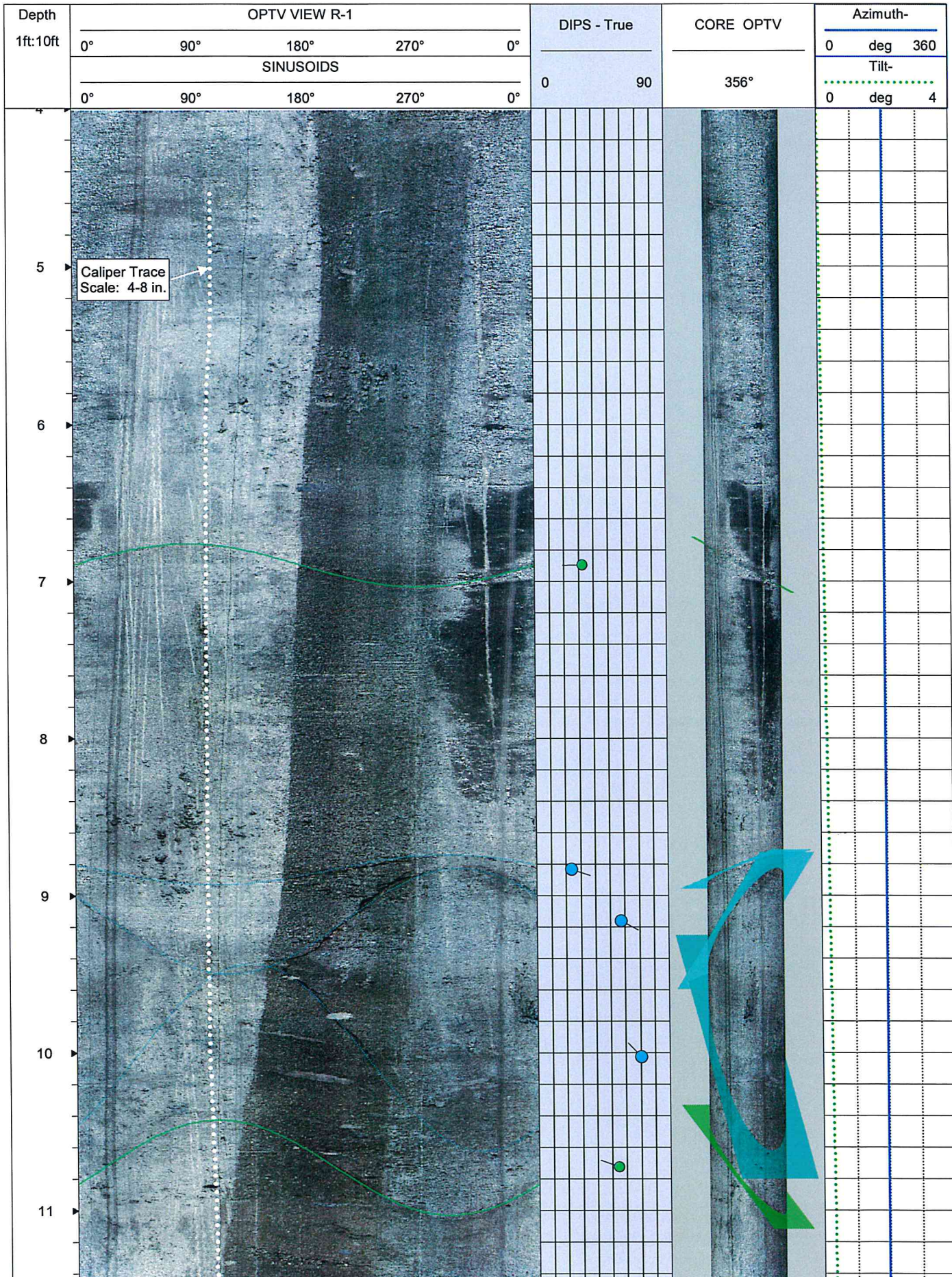


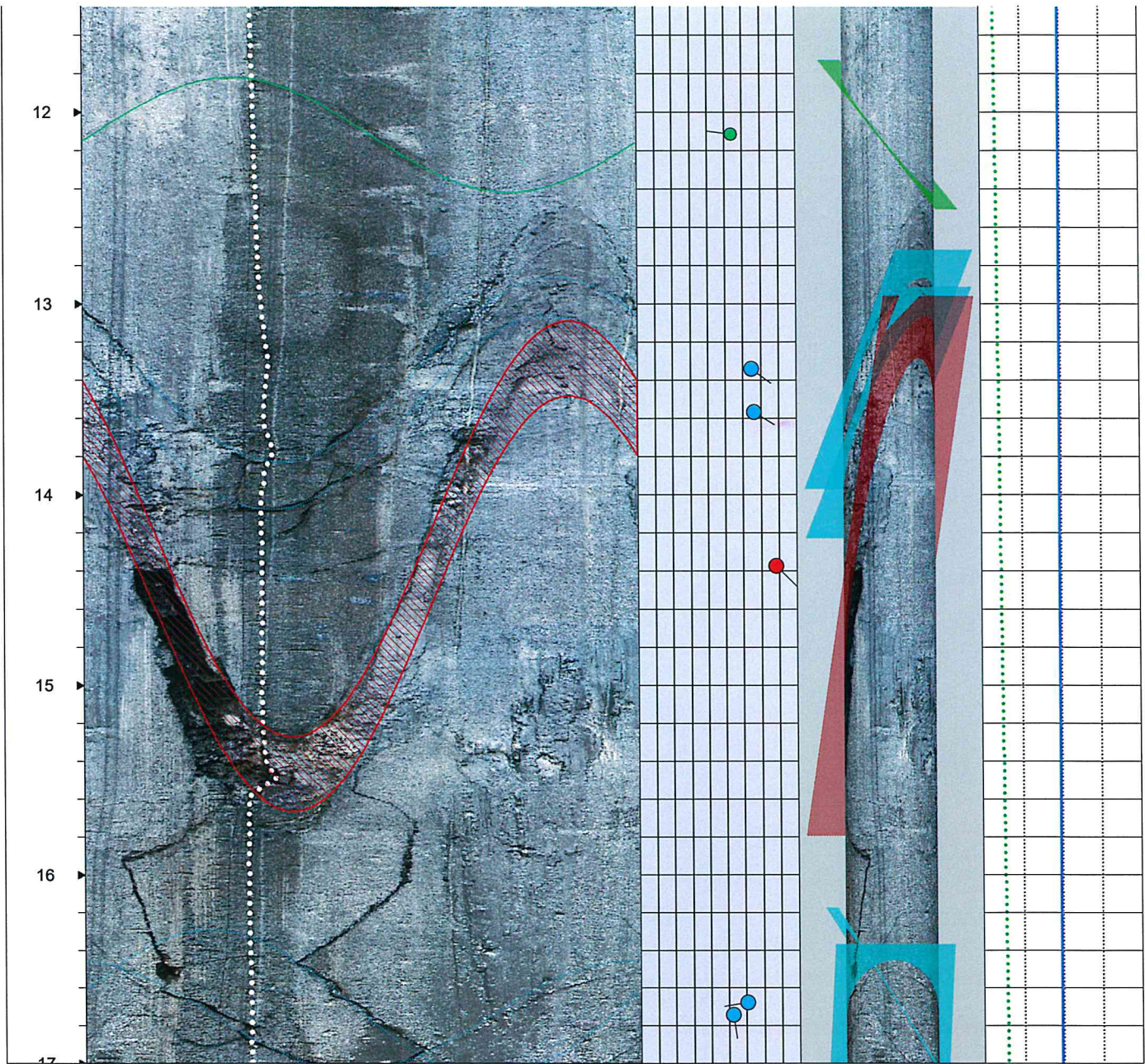
**TELEVIEWER
ANALYSIS OF
DIPS**

COMPANY: SHN
WELL ID: B-102
FIELD: EASTLAKE LANDFILL
COUNTY: LAKE

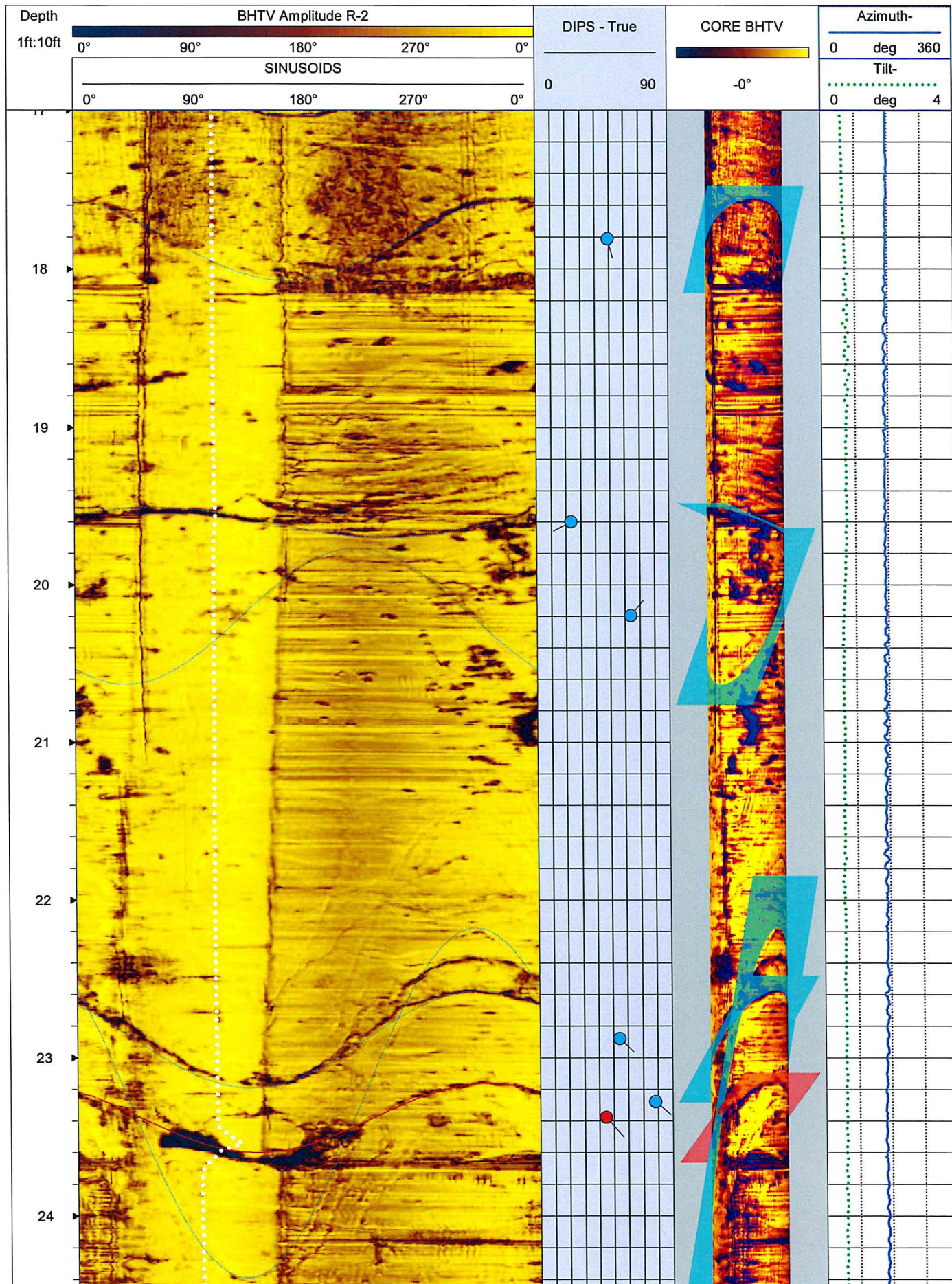
DATE: DEC. 21, 2017
CASING: PVC to 3-ft bgs
JOB NO. NS175076
STATE: CA

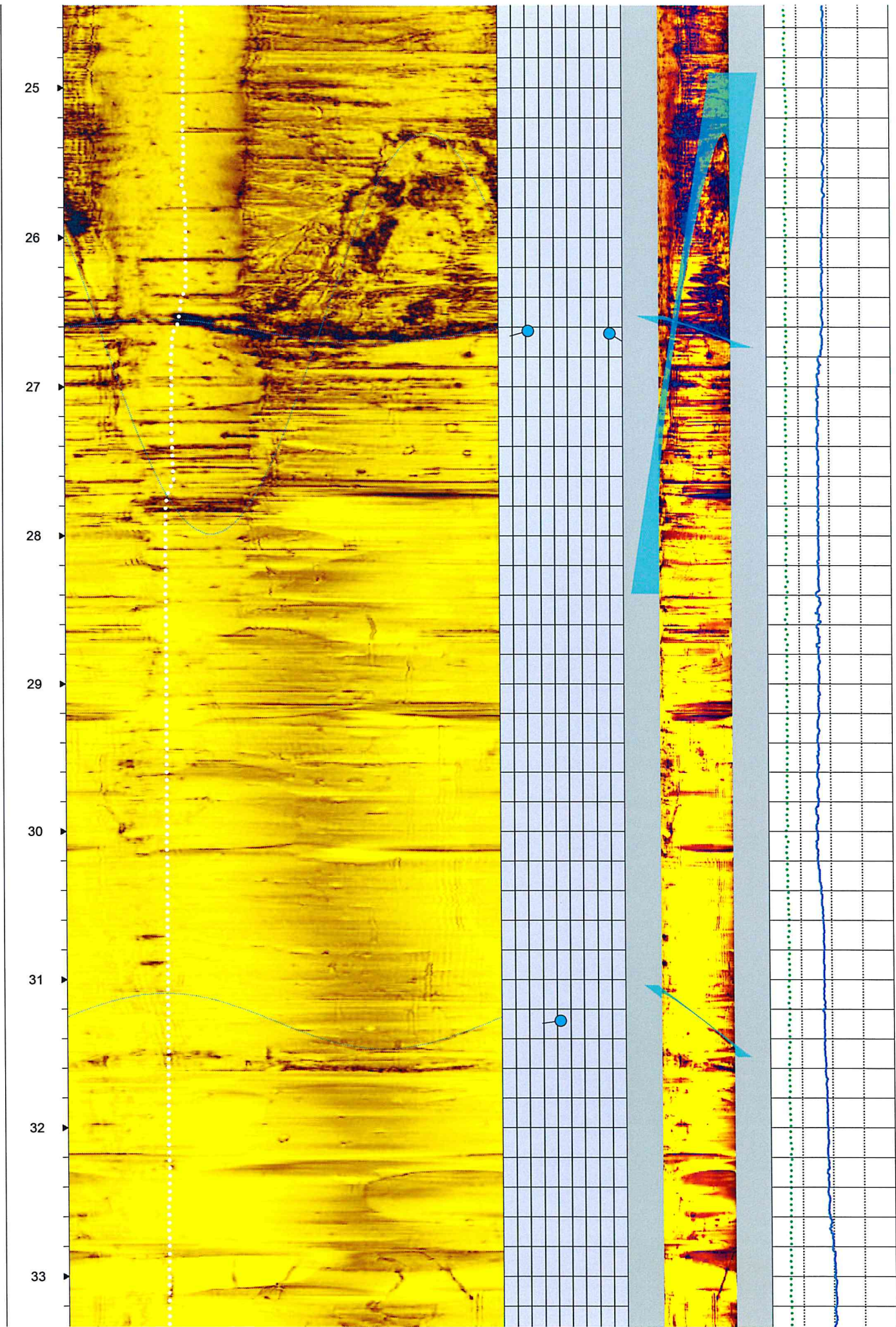
NOTES: Plot 1 of 2

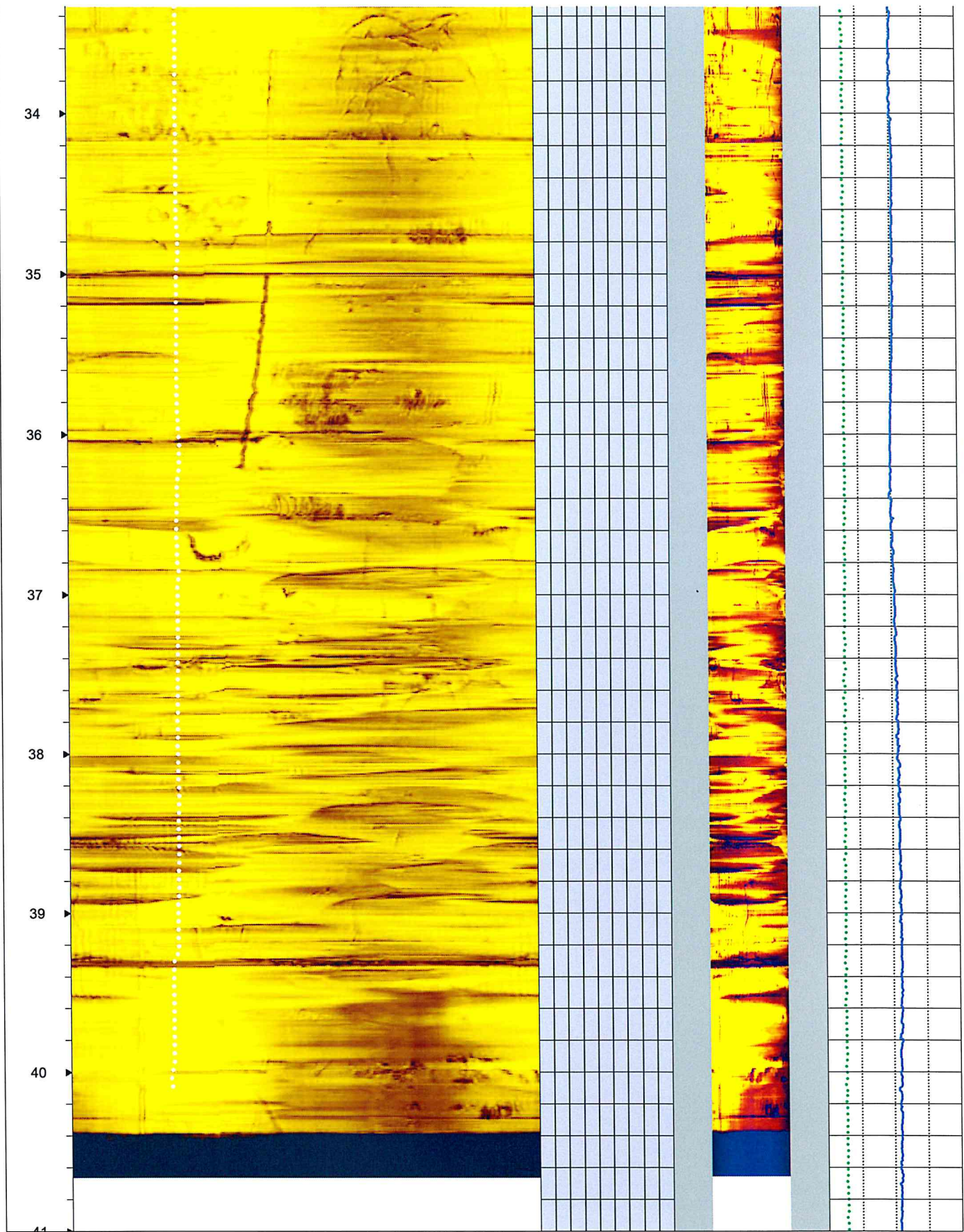




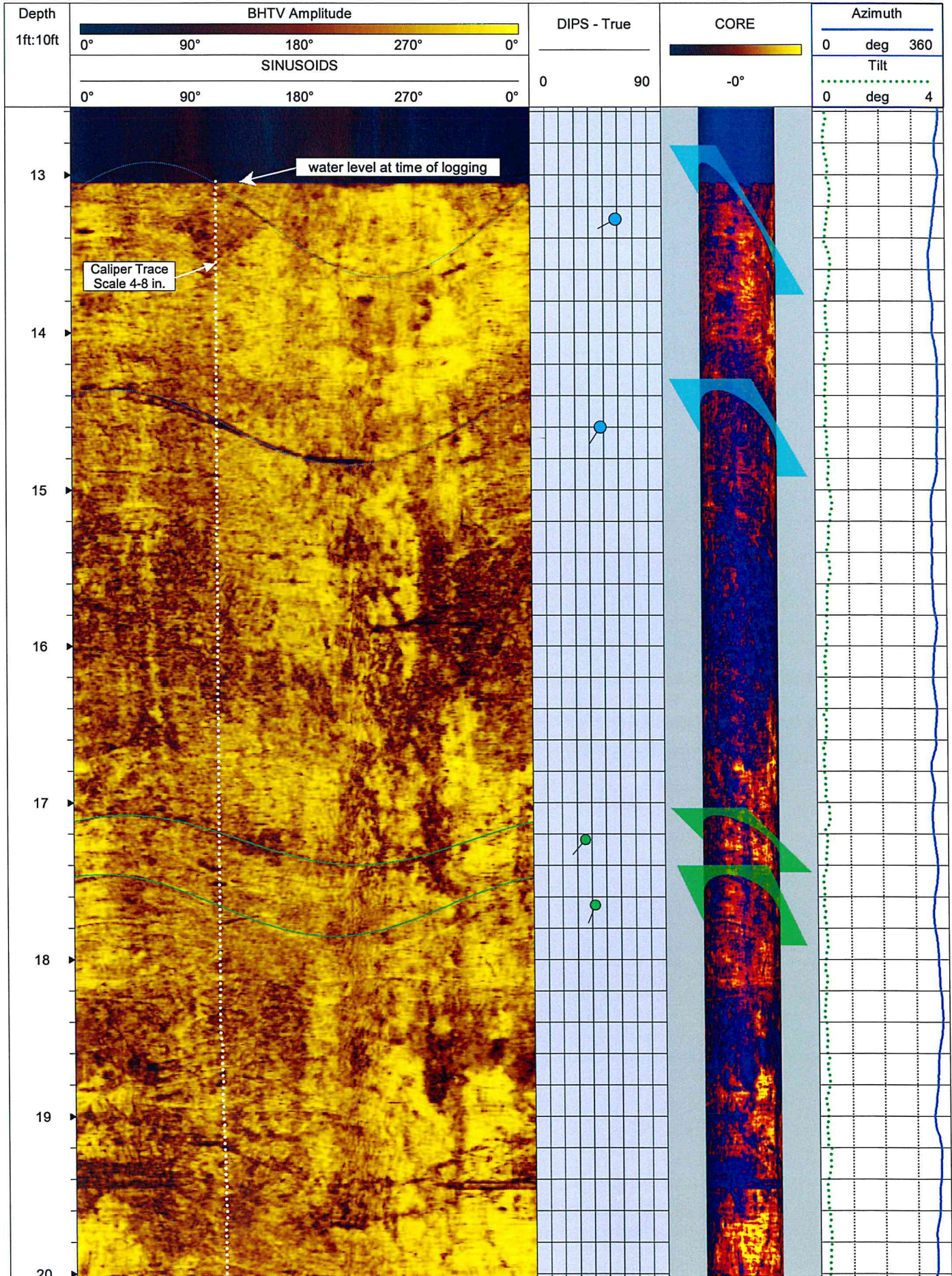
NOTES: Plot 2 of 2

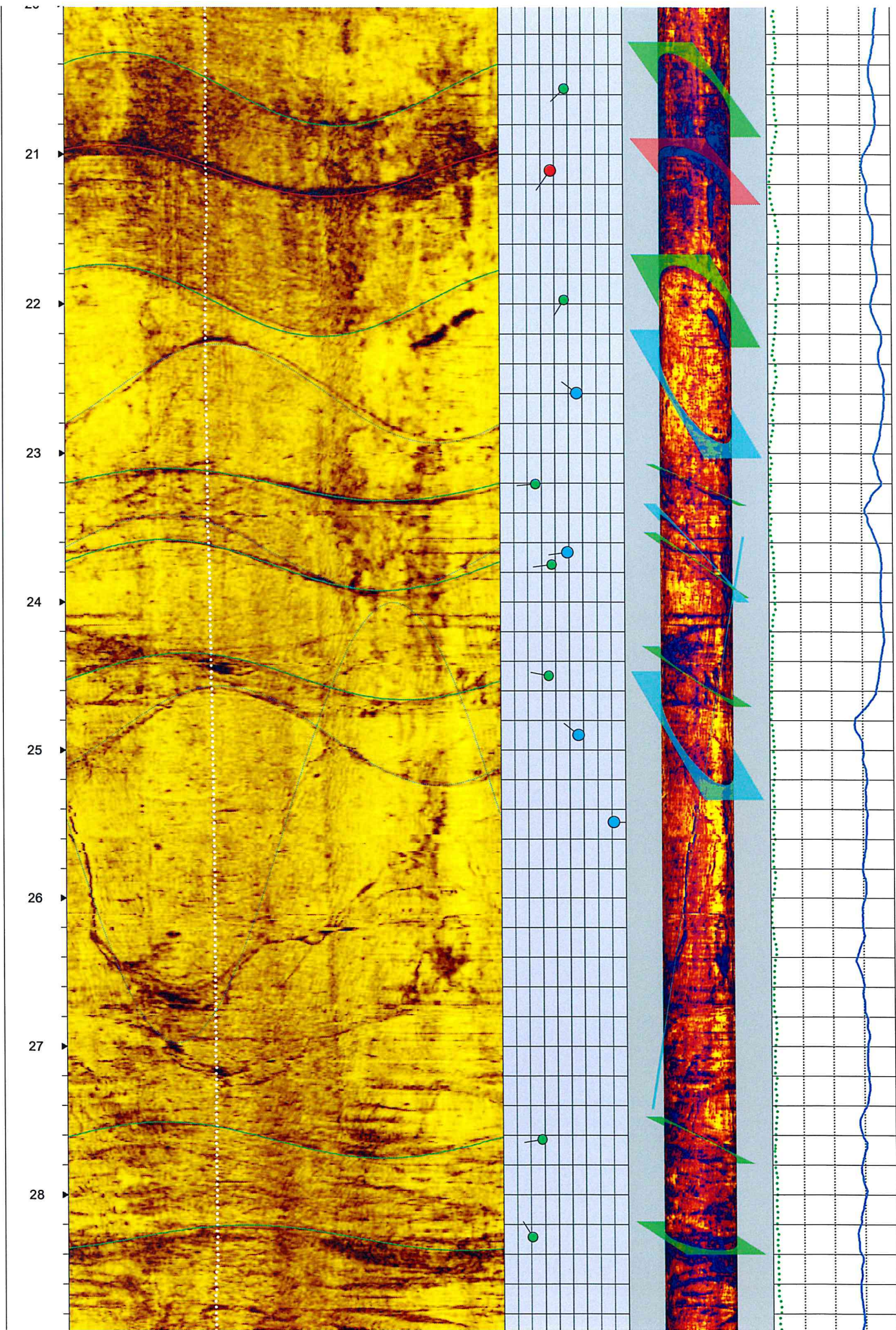


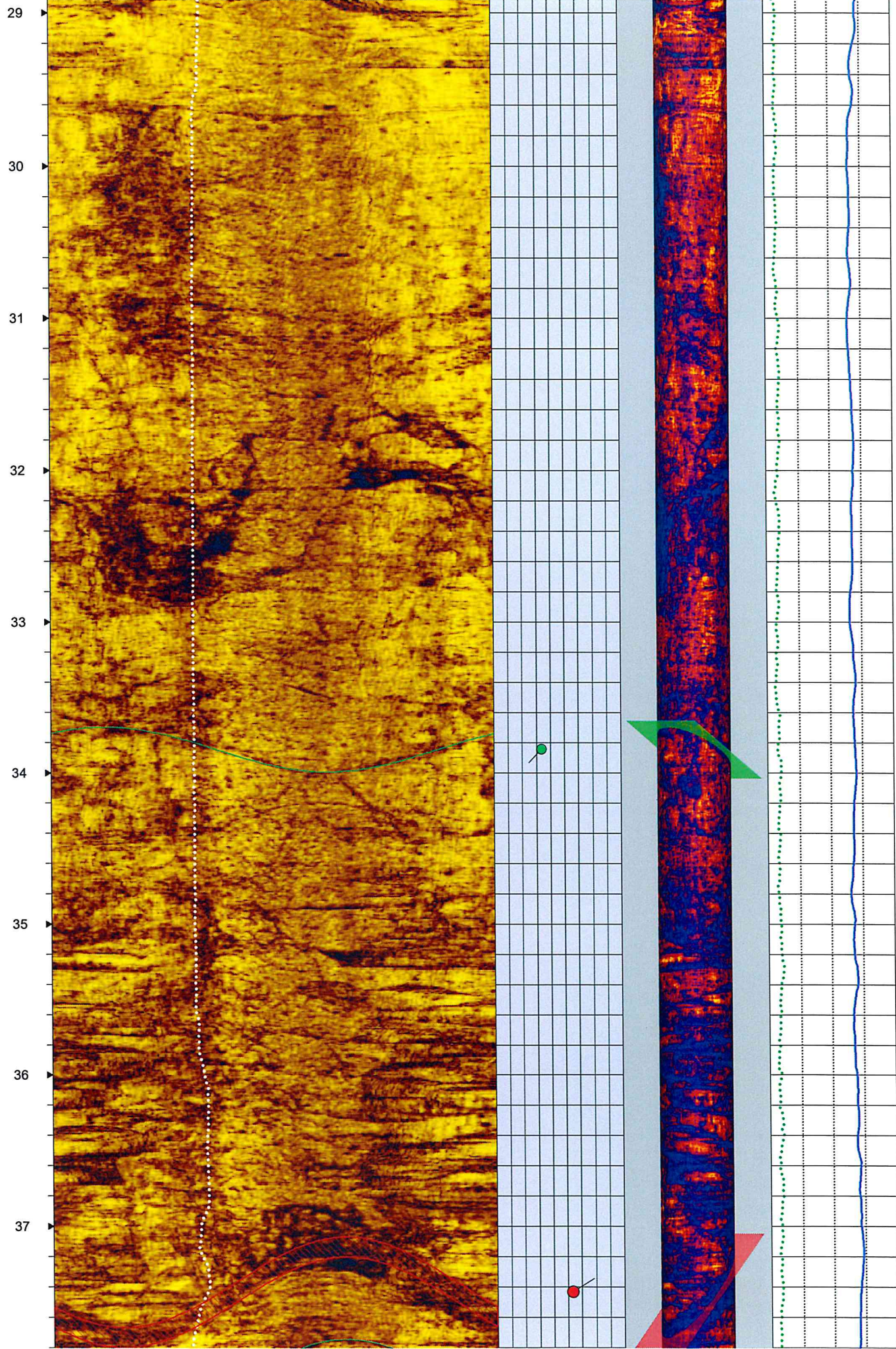


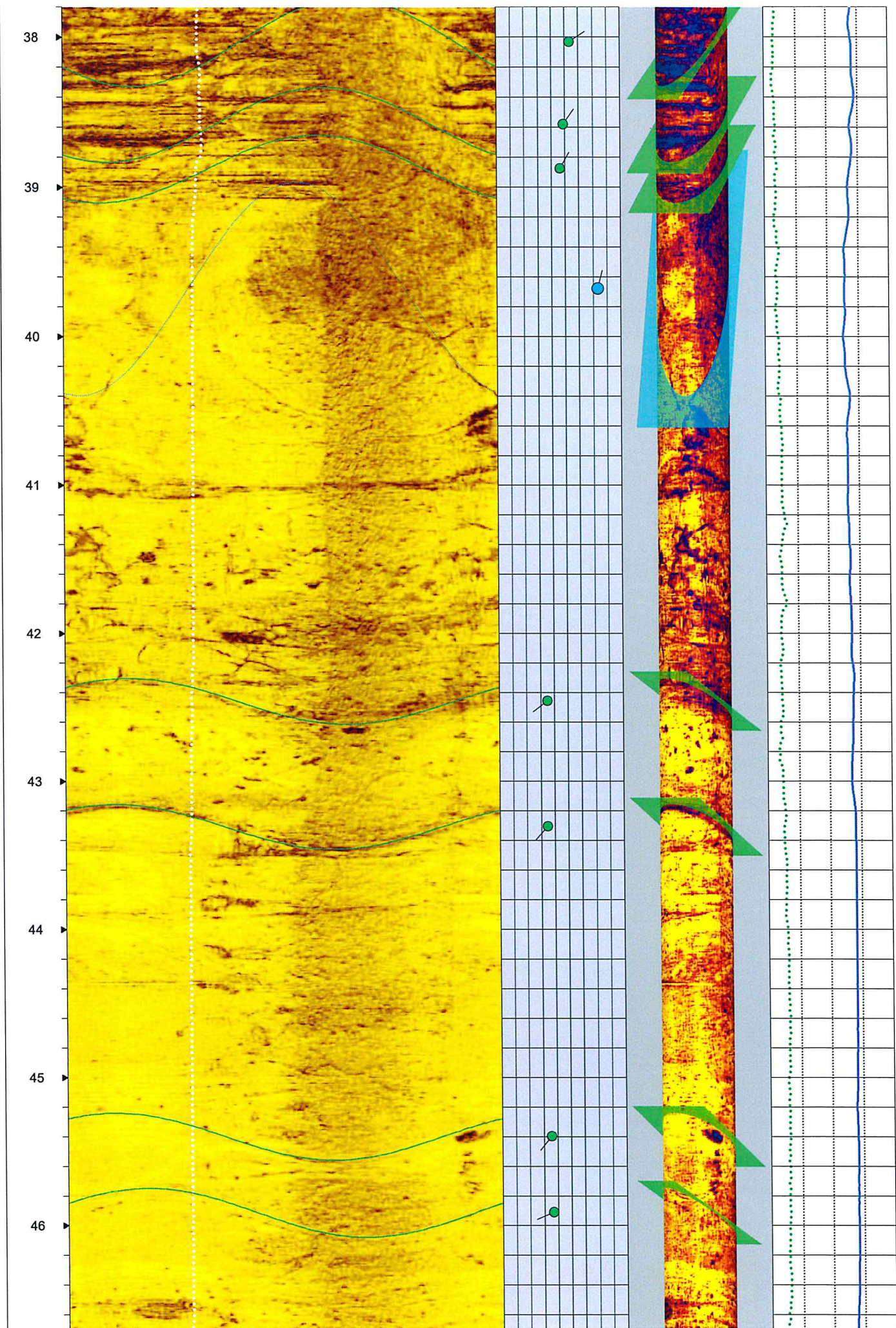


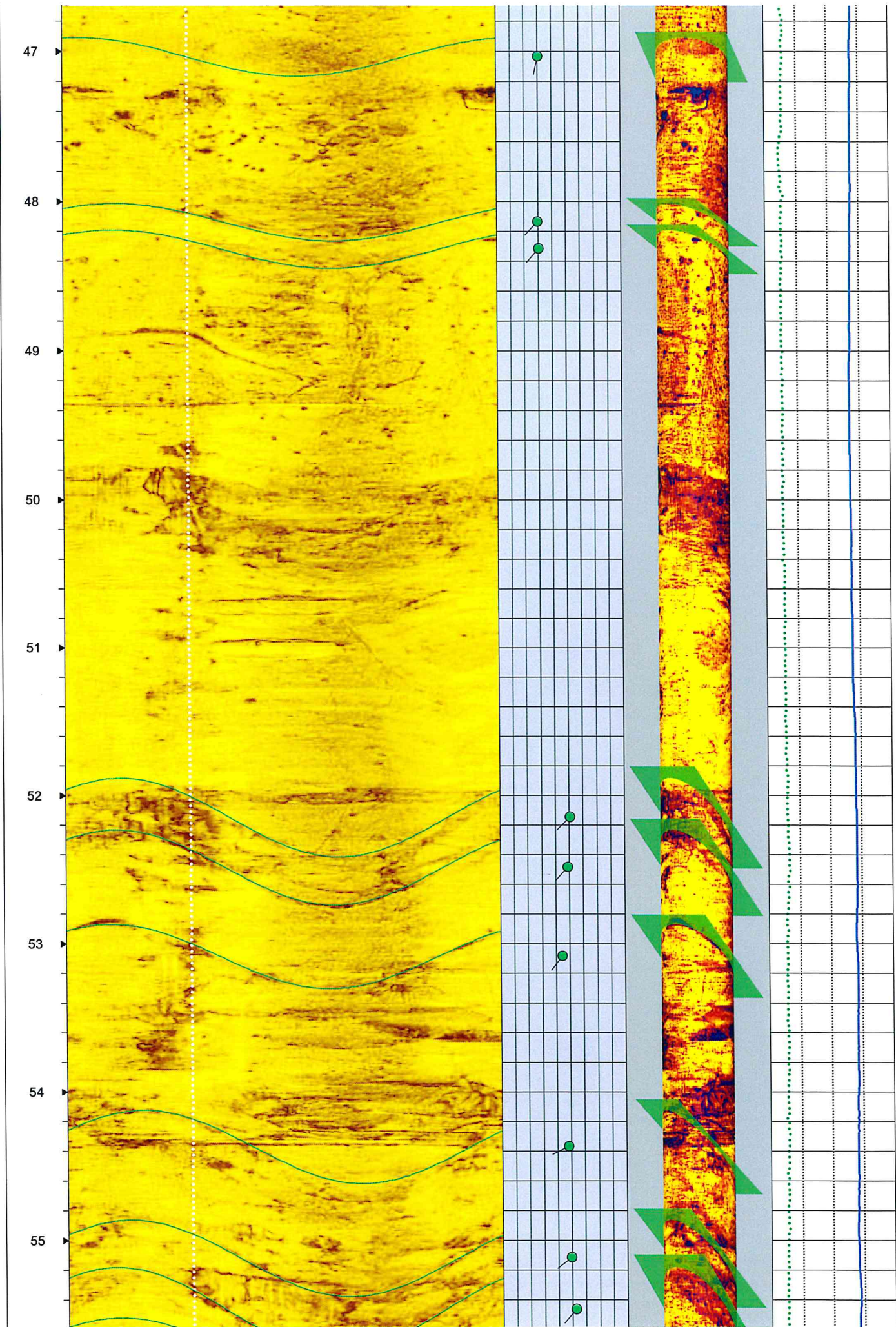
NOTES:











56

57

58

59

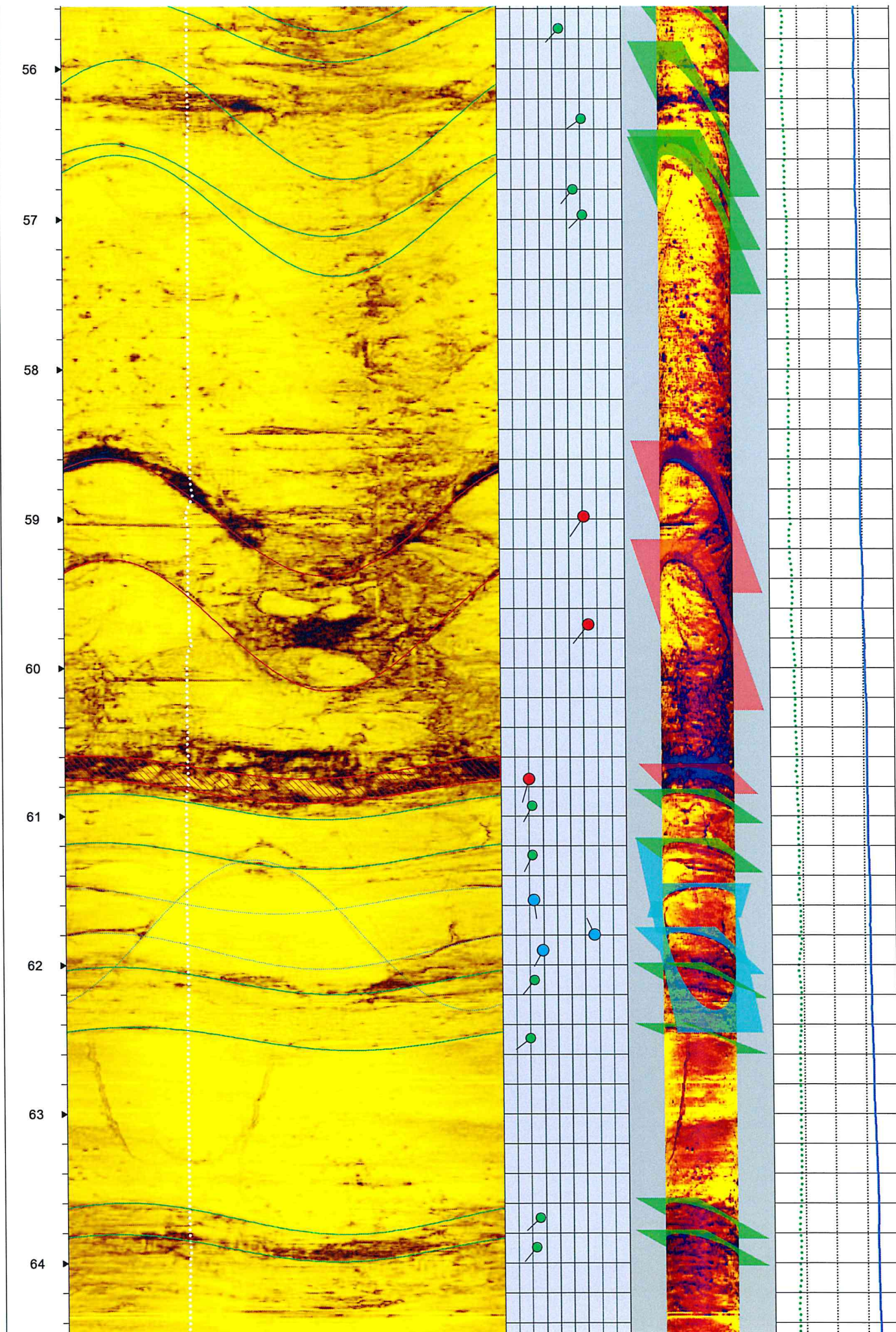
60

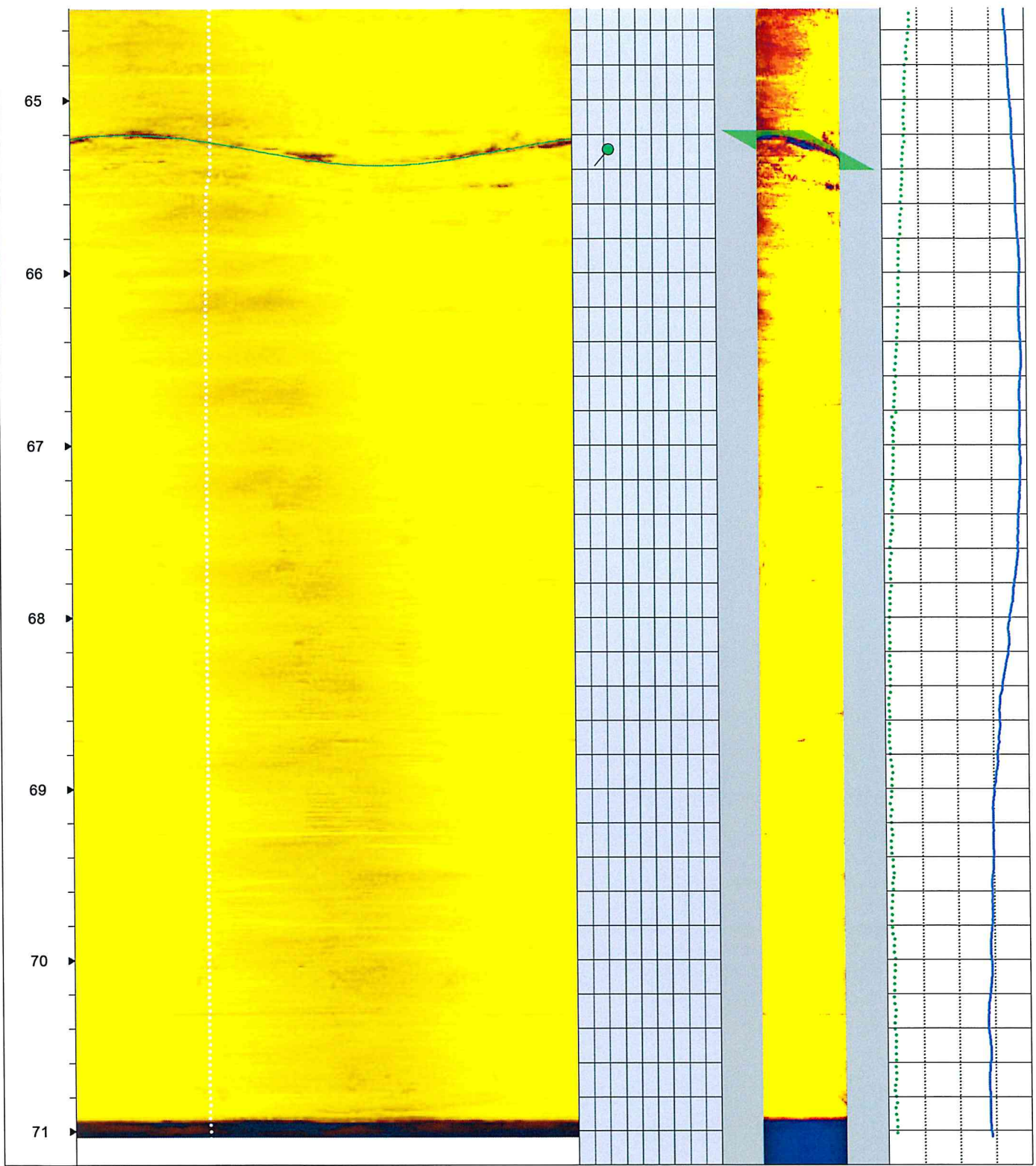
61

62

63

64





2

Seismic Refraction Survey

February 28, 2018

SHN Consulting Engineers & Geologists, Inc.
812 West Wabash Avenue
Eureka, California 95501

Subject: Seismic Refraction Survey:
Eastlake Landfill
Lake County, California

NORCAL Job # NS185005

Attention: Mr. Erik Nielsen

This report presents the findings of a seismic refraction (SR) survey performed by NORCAL Geophysical Consultants for SHN Consulting Engineers & Geologists, Inc. (SHN) at the Eastlake Landfill in Lake County, California. The survey was performed on January 30th and 31st, 2018 by NORCAL Professional Geophysicist David T. Hagin PGp No. 1033 and Senior Geophysical Technician Travis W. Black. Logistical support and field assistance were provided by the landfill manager, Mr. Kris Byrd.

1.0 SITE DESCRIPTION

The Eastlake Landfill facility straddles the eastern border of the city of Clearlake. The recycling facility is within the city limits and the active landfill area is just to the east of the city boundary. SHN is currently performing a feasibility evaluation for a possible expansion of the landfill to the south and southwest.

The site of the investigation is in the proposed expansion area, south and southwest of the active landfill. The area extends down a gently sloping dirt roadway and across a large cut pad, as shown on Plate 1. At the time of the survey the area was open and free from vegetation, and the ground surface was moist to wet from recent rains.

In the area of the cut pad, exposed rock appeared to be sandstone. The rock displayed grooves, apparently from the earth moving equipment used to cut the pad, and the rock broke apart easily by hand. These observations suggest that the rock is relatively soft at the surface, and may be highly weathered and/or poorly indurated. Available geologic maps indicate that the general area is underlain by Quaternary, Tertiary and Mesozoic sandstones, siltstones, shales and conglomerates (California Geological Survey, 2010).



Prior to this seismic refraction survey several exploratory borings were performed on site by SHN. Suspension P- and S-Wave velocity logging was completed on Borehole B-103 by NORCAL in December, 2017. The location of Borehole B-103 is shown on Plate 1 and Plate 2.

2.0 PURPOSE

The purpose of the SR survey is to measure lateral and vertical variations in the primary seismic wave velocity of the subsurface within the area of investigation. This information can be used to evaluate the thickness of overburden, the depth to rock and general bedrock excavation characteristics (rippability). Knowledge of these parameters is necessary prior to the proposed landfill expansion.

3.0 SEISMIC REFRACTION METHOD

The SR method can be used to determine the compressional wave velocity of subsurface materials. Compressional waves, also known as primary or "P" waves, are dependent on physical properties such as hardness, compaction, and induration. However, other factors such as bedding, fracturing and saturation also affect P-wave velocity (V_p). Detailed descriptions of the SR methodology, our data acquisition and analysis procedures, the instrumentation we used and general limitations of the method are provided in Appendix A.

4.0 RESULTS

SR data were collected along the 1,260 foot long transect shown in red on Plate 1. The results of the survey are illustrated by the seismic velocity cross-section (profile) shown on Plate 2. The vertical axis represents elevation and the horizontal axis represents survey stationing (distance along the line). The solid dark line along the top of the profile indicates the ground surface. V_p is represented by the labeled contours and color shading between contours. The relationship between color and V_p is specified by the color scale shown at the bottom of the plate.

5.0 SEISMIC VELOCITY VALUES

The V_p measured by the seismic refraction survey range from about 2,000-feet per second (ft/sec) at the surface to just over 9,000-ft/sec at depth. This velocity range can be differentiated into three sub-ranges which we define herein as low, moderate and high. Low V_p range from 2,000- to 5,000-ft/sec and are represented by tan to yellow shading. V_p in this range typically represent surficial soils and poorly consolidated sedimentary deposits with relatively low

moisture content. Moderate Vp range from 5,000- to 7,000-ft/sec and are represented by green and blue shading. Vp in this range probably represent more consolidated, cemented or saturated sediments or possibly deeply weathered or poorly indurated rock. High Vp range from 7,000- to 9,000-ft/sec and are represented by varying shades of maroon. For the most part these velocities probably represent bedrock in various degrees of weathering where the degree of weathering and/or fracturing decreases with increased Vp.

6.0 DISCUSSION

6.1 SR PROFILE

The SR profile for Line 1 shows significant variability in the depth to the various velocity ranges defined in Section 5.0. These variations are represented by the undulating velocity contours that occur primarily between Station 0 and Station 950, and suggest variation of geologic conditions along the profile. The noted variations may include changes in rock depth, type and condition, as well as variations in the degree of weathering and/or fracturing. In contrast, the velocity layers between Station 950 and Station 1260 appear relatively consistent in depth.

Specifically, the low Vp zone is especially variable on the southwest portion of the profile, approximately between Station 0 and Station 850. A majority of this area is within the large cut pad. The profile shows a surficial low Vp zone nearly absent in some locations to approximately 20 feet thick in others. The underlying moderate Vp zone is also quite variable, ranging from 10 to 30 feet in thickness. These values suggest shallow to deep weathering and/or poorly indurated rock within the upper 5 to 30 feet. There appears to be considerable variability in depth of weathering on the southwestern two-thirds of the line, where rock is exposed on the cut pad; whereas, the northeast third along the road is relatively consistent. High Vp values suggestive of more competent rock are noted as shallow as 17 feet near Station 450 and as deep as 58 feet near Station 840. The maximum Vp shown on the profile are slightly greater than 9,000 ft/s, and appear as shallow as 40 feet within a relatively small zone near Station 450.

6.2 SUSPENSION LOGGING COMPARISON

A comparison of the results of the suspension P-wave logging performed in Borehole B-103 to the seismic refraction profile shows good correlation. Generally, the suspension log indicates moderate Vp of 5,000 ft/s to 7,000 ft/s within the upper 50 feet and an increase in values to over 8,000 ft/s below 50 feet depth.

7.0 RIPPABILITY ASSESSMENT

Seismic velocity can be used to assess the excavatability (rippability) of rock materials based on empirical data. Charts relating Vp to excavation characteristics have been developed from field tests by others. These charts list the seismic velocity of various types of rock and their relative ease of excavation using different types of ripping equipment.

Caterpillar Tractor Company publishes a performance manual that lists ripper performance charts for the D8, D9, D10 and D11 series tractors. Although the equipment to be used may vary from the models listed, the charts may still provide a relative guide to aid in characterizing rippability. The information presented in Table A is taken from the ripper performance charts contained in the Caterpillar Performance Handbook (Caterpillar, Edition 36, April 2006) for the tractors listed above operating in sandstone:

Table A: Seismic P-Wave Velocity and General Rippability in Sandstone

Equipment Model	Rippable Velocity (ft/sec)	Marginal Velocity (ft/sec)	Non-Rippable Velocity (ft/sec)
D8	<6,300	6,300 to 8,500	>8,500
D9	<7,500	7,500 to 9,600	>9,600
D10	<8,500	8,500 to 10,800	>10,800
D11	<9,800	9,800 to 12,000	>12,000

Based on the seismic profiles and the proposed depth of excavations it may be possible to determine the size of the equipment that will likely be required. If excavations are planned where even the largest equipment indicates non-rippable conditions alternate methods may be required for excavation. It is noted that all of the survey indicates rock that falls into the rippable or marginal category for Model D9 and larger, based on the sandstone category.

This information should only be used as a general guide to rippability as many other factors also contribute to the evaluation of rock rippability. These factors include rock jointing and fracture patterns, the experience of the equipment operator, and the equipment and excavation methods selected.

8.0 LIMITATIONS

It should be noted that the seismic refraction technique is based on the assumption that seismic velocity increases with depth. Any layers representing a decrease in velocity with depth, otherwise known as a velocity inversion, will not be defined and will result in the over-estimation of the depth of deeper, higher velocity layers. In addition, relatively thin layers might not be individually resolved and might, instead, be lumped together with other layers. Hard and soft zones within a given seismic layer will tend to be averaged into the velocity of that layer. There is not necessarily a one-to-one relationship between lithologic layers and seismic layers. It is entirely possible that two different types of material could have the same seismic velocity. Alternatively, a change in velocity can occur within a single lithologic unit.

Since the accuracy of our findings is subject to the limitations described above, it should be noted that subsurface conditions may vary from those depicted in the final results. A more detailed discussion of the limitations with regard to the seismic refraction method is presented in Appendix A.

9.0 STANDARD OF CARE

The scope of NORCAL's services for this project consisted of using geophysical methods to characterize the subsurface. The accuracy of our findings is subject to specific site conditions and limitations inherent to the techniques used. We performed our services in a manner consistent with the standard of care ordinarily exercised by members of the profession currently employing similar methods. No warranty, with respect to the performance of services or products delivered under this agreement, expressed or implied, is made by NORCAL.

SHN Consulting Engineers & Geologists, Inc.
February 28, 2018
Page 6



We appreciate the opportunity to participate on this project. If you have any questions or require additional geophysical services, please do not hesitate to call on us.

Sincerely,

NORCAL Geophysical Consultants, Inc.

A handwritten signature in blue ink that reads "David T. Hagin".

David T. Hagin
Professional Geophysicist PGp 1033



DTH/WEB/tt

Enclosures: Plates 1 and 2
Appendix A - Seismic Refraction

Appendix A
SEISMIC REFRACTION

APPENDIX A

SEISMIC REFRACTION (SR) SURVEY

1.0 METHODOLOGY

The seismic refraction method provides information regarding the seismic velocity structure of the subsurface. An impulsive (mechanical or explosive) source is used to produce compressional (P) wave seismic energy. The P-waves propagate into the earth and are refracted along interfaces caused by an increase in velocity. A portion of the P-wave energy is refracted back to the surface where it is detected by sensors (geophones) that are coupled to the ground surface in a collinear array (spread). The detected signals are recorded on a multi-channel seismograph and are analyzed to determine the shot point-to-geophone travel times. These data can be used along with the corresponding shot point-to-geophone distances to determine the depth, thickness, and velocity of subsurface seismic layers.

The seismic refraction technique is based on several assumptions. Paramount among these are that seismic velocity:

- 1) Increases with depth, and,
- 2) is uniform within each layer over the length of the given spread.

In cases where these assumptions do not hold, the accuracy of the technique decreases. For example, if a low velocity layer occurs between two layers of higher velocity, the low velocity layer will not be detected and the depth to the underlying high velocity layer will be erroneously large. Also, if the velocity of a seismic layer varies laterally within a spread, those variations will be interpreted as fluctuations in the elevation of the underlying seismic layer.

2.0 DATA ACQUISITION/INSTRUMENTATION

We collected SR data from a single seismic line, labeled Line 1 and shown in red on Plate 1. In order to achieve the desired length of 1,260 feet, the line was acquired as 5 overlapping spreads. Each spread was composed of 24-geophones and 5-shot points distributed in a collinear array, as shown in Figure 1. This distribution of the geophones and shot points resulted in a total length (end shot point to end shot point) of 300 feet for each spread. The seismic line was positioned within the area to the south and southeast of the active landfill described in section 1.0 of this report. Seismic energy was produced at each shot point by multiple impacts with a 16# sledge hammer against a metal strike plate on the ground surface.

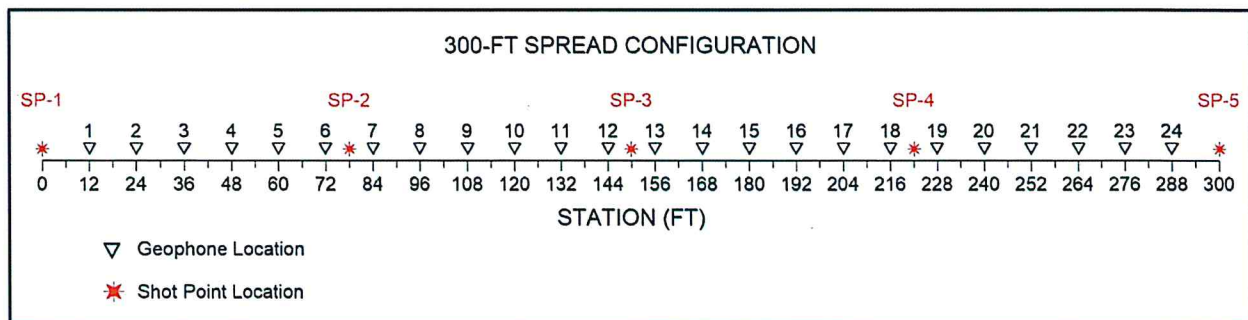


Figure 1: Distribution of shot points and geophones along the first spread of Line 1. All additional spreads are similar except that the shot points and geophone locations are numbered differently (in sequential order).

The seismic waveforms produced at each shot point were recorded using a Geometrics **Geode** 24-channel engineering distributed array seismograph and Oyo **Geospace** geophones with a natural frequency of 8-Hz. The seismic waveforms were digitized, processed and amplified by the Geode and transmitted via a ruggedized Ethernet cable to a field computer. There the data were archived for subsequent processing and displayed on the computers LCD screen in the form of seismograms. These were subsequently used to determine the time required for P-waves to travel from each shot point to each geophone in a given array (spread).

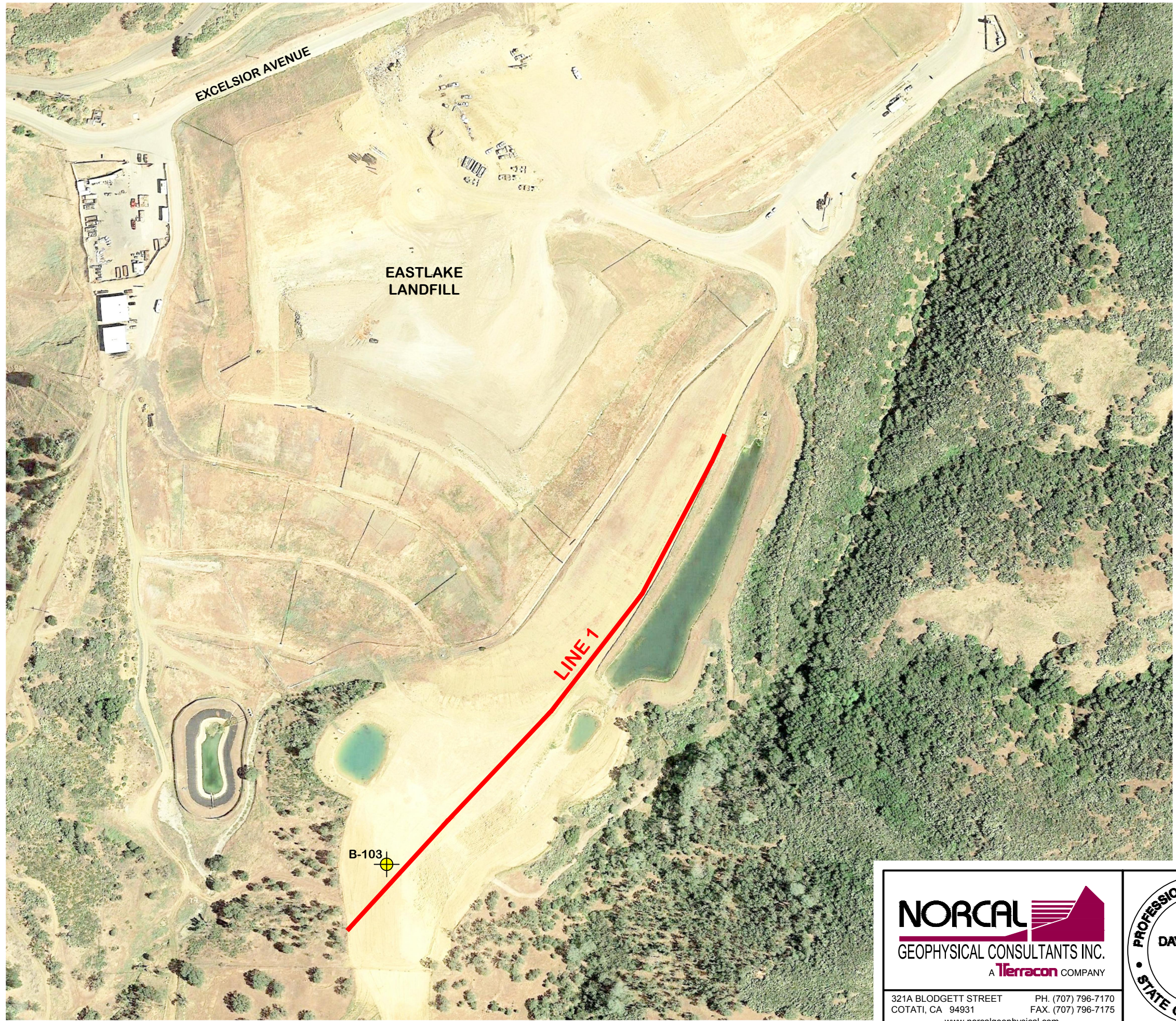
3.0 DATA ANALYSIS

The seismic refraction data were processed using the software package **Seislmager** which was written by Oyo Corporation (Japan) and distributed by Geometrics Inc. The first stage of seismic refraction processing included compilation and identification of first arriving P-wave energy at each geophone from each shot point. This process was conducted using **Pickwin, Version 5.1.1.2** (2013), which is part of the **Seislmager** package. A second interactive program **Plotrefa, Version 3.0.0.6** (2014) was used to assign surface elevations to each geophone and velocity layer assignments to the travel times. We then used **Seislmager's** time-term routine to compute a basic 2D seismic velocity model based on these inputs. This model served as input to **Seislmager's** tomographic routine which produced a more refined, more detailed final model. The data from the tomographic model were then input to the graphic program **Surfer 13.5.583** to construct a 2D cross-section (profile) illustrating variations in seismic velocity versus depth and distance beneath the seismic line. On this profile the horizontal axis represents distance (Station) in feet from the west end of the line and the vertical axis represents elevation in feet above mean sea level. Labeled contours indicate the seismic velocity at various depths. In addition, color shading between the contours indicates velocity according to the color bar shown at the bottom of each plate.

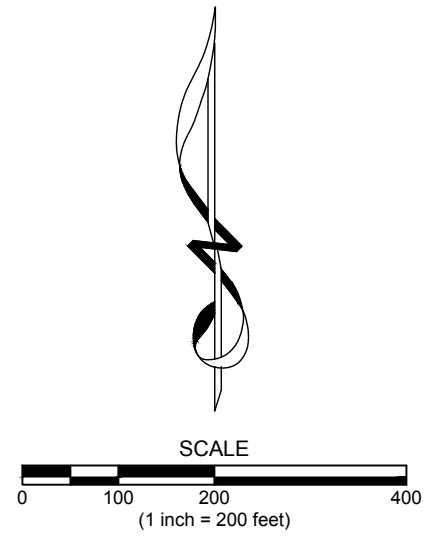
4.0 LIMITATIONS

In general, there are limitations unique to the SR method. These limitations are primarily based on assumptions that are made by the data analysis routine. First, the data analysis routine assumes that the velocities along the length of each spread are uniform. If there are localized zones within each layer where the velocities are higher or lower than indicated, the analysis routine will interpret these zones as changes in the surface topography of the underlying layer. A zone of higher velocity material would be interpreted as a low in the surface of the underlying layer. Zones of lower velocity material would be interpreted as a high in the underlying layer.

Second, the data analysis routine assumes that the velocity of subsurface materials increases with depth. Therefore, if a layer exhibits velocities that are slower than those of the material above it, the slower layer will not be resolved. Also, a velocity layer may simply be too thin to be detected. Due to these and other limitations inherent to the SR method, the results of the SR survey should be considered only as approximations of the subsurface conditions. The actual conditions may vary locally. Other independent data (e.g., surface and borehole geology) should be integrated with SR data to enhance the subsurface interpretation.



VICINITY MAP



LEGEND	
	SEISMIC REFRACTION LINE
	BORING

NORCAL
GEOPHYSICAL CONSULTANTS INC.
A Terracon COMPANY

321A BLODGETT STREET
COTATI, CA 94931
www.norcalgeophysical.com

PH. (707) 796-7170
FAX. (707) 796-7175

PROFESSIONAL GEOPHYSICIST
DAVID T HAGIN
No. 1033
STATE OF CALIFORNIA

SITE LOCATION MAP
EASTLAKE LANDFILL
SEISMIC REFRACTION SURVEY

LOCATION: LAKE COUNTY, CALIFORNIA

CLIENT: SHN CONSULTING ENGINEERS & GEOLOGISTS, INC.

JOB #: NS185005

DATE: FEBRUARY 2018

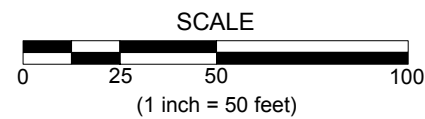
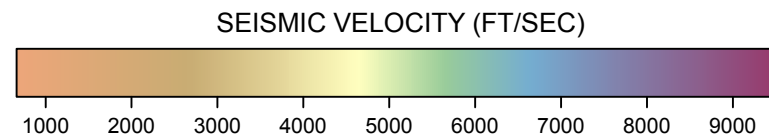
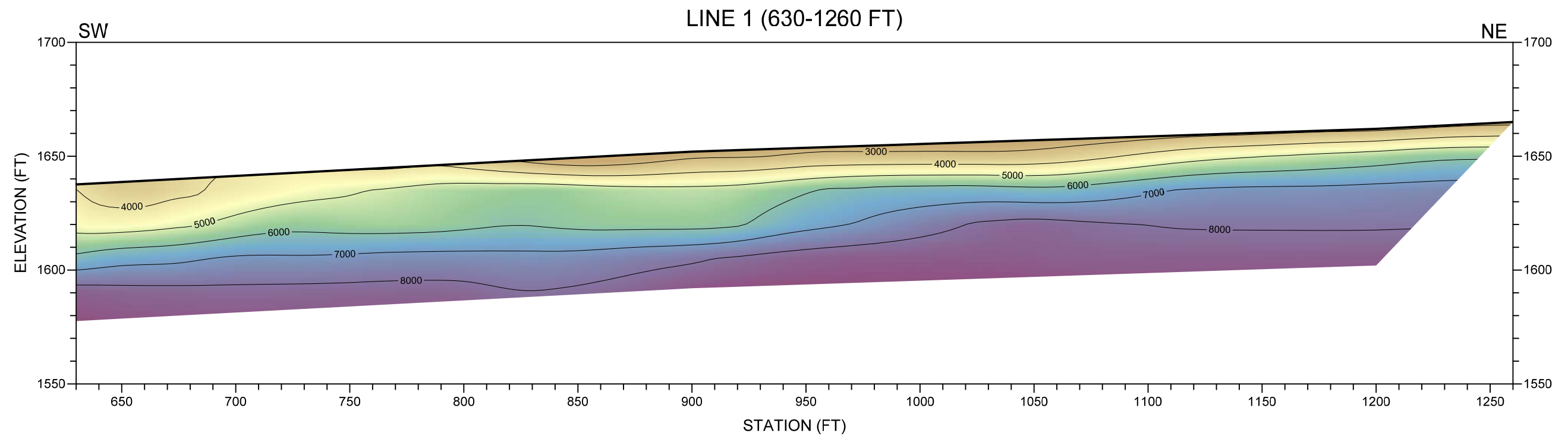
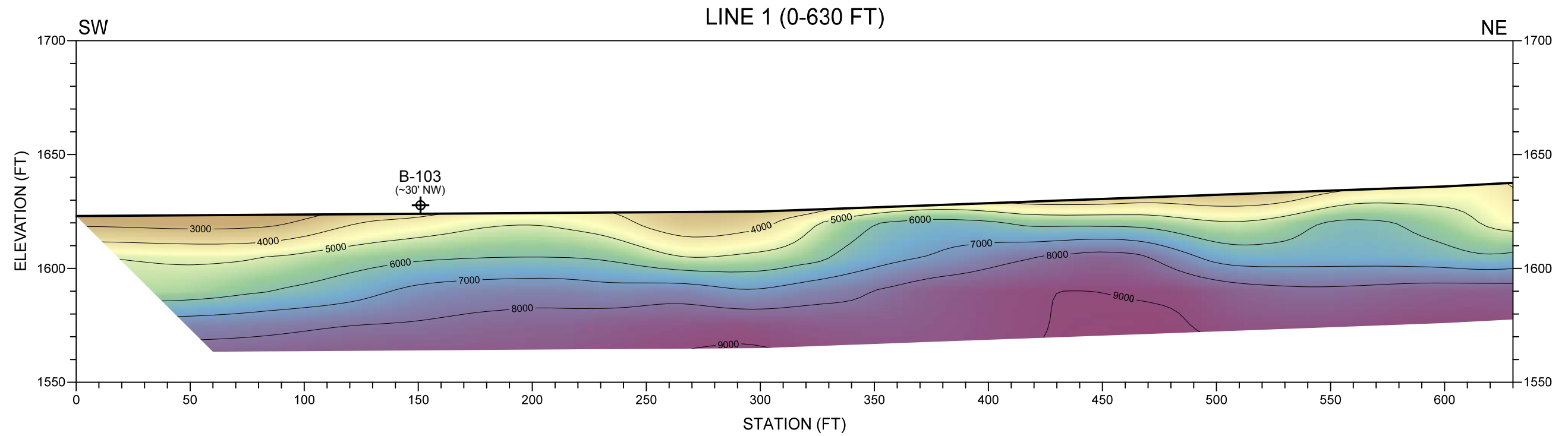
DRAWN BY: G.RANDALL

APPROVED BY: DTH

David Hagin

2/28/2018

PLATE
1



LEGEND	
	BORING

NORCAL
GEOPHYSICAL CONSULTANTS INC.
A Terracon COMPANY

321A BLODGETT STREET PH. (707) 796-7170
COTATI, CA 94931 FAX. (707) 796-7175
www.norcalgeophysical.com

PROFESSIONAL GEOPHYSICIST
DAVID T HAGIN
No. 1033
STATE OF CALIFORNIA

SEISMIC REFRACTION PROFILE LINE 1 EASTLAKE LANDFILL		
LOCATION: LAKE COUNTY, CALIFORNIA		
CLIENT: SHN CONSULTING ENGINEERS & GEOLOGISTS, INC.		
JOB #: NS185005	DATE: FEBRUARY 2018	PLATE 2
DRAWN BY: G.RANDALL	APPROVED BY: DTH	
<i>David Hagin</i> 2/28/2018		